



# University of HUDDERSFIELD

## University of Huddersfield Repository

Barber, Jennifer

Adrenomedullin Receptor Antagonists as a Potential Therapeutic Target for Major Depressive Disorder

### Original Citation

Barber, Jennifer (2018) Adrenomedullin Receptor Antagonists as a Potential Therapeutic Target for Major Depressive Disorder. Masters thesis, University of Huddersfield.

This version is available at <http://eprints.hud.ac.uk/id/eprint/35114/>

The University Repository is a digital collection of the research output of the University, available on Open Access. Copyright and Moral Rights for the items on this site are retained by the individual author and/or other copyright owners. Users may access full items free of charge; copies of full text items generally can be reproduced, displayed or performed and given to third parties in any format or medium for personal research or study, educational or not-for-profit purposes without prior permission or charge, provided:

- The authors, title and full bibliographic details is credited in any copy;
- A hyperlink and/or URL is included for the original metadata page; and
- The content is not changed in any way.

For more information, including our policy and submission procedure, please contact the Repository Team at: [E.mailbox@hud.ac.uk](mailto:E.mailbox@hud.ac.uk).

<http://eprints.hud.ac.uk/>

# **Adrenomedullin Receptor Antagonists as a Potential Therapeutic Target for Major Depressive Disorder**

**Jennifer Aislinn Barber BSc (Hons)**

**A thesis submitted to the University of Huddersfield in partial fulfilment of  
the requirements for the degree of Masters by Research in Pharmaceutical  
Sciences**

**University of Huddersfield**

**September 2018**



## **Copyright Statement**

The following notes on copyright and the ownership of intellectual property rights must be included as written below:

- i. The author of this thesis (including any appendices and/ or schedules to this thesis) owns any copyright in it (the "Copyright") and s/he has given The University of Huddersfield the right to use such Copyright for any administrative, promotional, educational and/or teaching purposes.
- ii. Copies of this thesis, either in full or in extracts, may be made only in accordance with the regulations of the University Library. Details of these regulations may be obtained from the Librarian. Details of these regulations may be obtained from the Librarian. This page must form part of any such copies made.
- iii. The ownership of any patents, designs, trademarks and any and all other intellectual property rights except for the Copyright (the "Intellectual Property Rights") and any reproductions of copyright works, for example graphs and tables ("Reproductions"), which may be described in this thesis, may not be owned by the author and may be owned by third parties. Such Intellectual Property Rights and Reproductions cannot and must not be made available for use without permission of the owner(s) of the relevant Intellectual Property Rights and/or Reproductions.



## Abstract

Major Depressive Disorder (MDD) is one of the most common mental health disorders in the world and yet, current treatments for MDD are very ineffective. There is an urgent need to find novel treatments with increased efficacy and reduced side effects. Increased levels of adrenomedullin (ADM), a short vasodilator peptide, are found in the blood of MDD patients. There are currently no known small molecular inhibitors of the two ADM receptors, ADM<sub>1</sub> and ADM<sub>2</sub>. We procured seven small molecular compounds capable of antagonising the ADM<sub>2</sub> receptor, from the European Lead Factory. These compounds were selected by high throughput screening. The ability of the compounds to block different pathways involved in ADM signalling was assessed. The most canonical pathway for ADM signalling is the activation of adenylate cyclase to increase intracellular cAMP. Measurements of intracellular ATP concentration revealed promising results for two of the compounds, TC14 and TC02. SKNSH cells pre-treated with 100 µM of these antagonist compounds and then treated with 1 µM of ADM peptide agonist had reduced cAMP, compared with cells treated with 1 µM of ADM agonist only. Pre-treatment with TC14 and TC02 resulted in intracellular cAMP concentrations of 0.7 nM and 5.3 nM, respectively, compared to a cAMP concentration of 31.3 nM in cells treated only with ADM agonist. We suggest that these compounds can be used in further research into the role of ADM in MDD. The hypothesis that some of the effects mediated by ADM, in health and disease, are dependent on the phosphorylation and inhibition of the transcription factor FoxO3a, via PI3K/Akt signalling, was also investigated.



## List of Abbreviations

---

ADM	Adrenomedullin
AMBP-1	Adrenomedullin Binding Protein 1
APS	Ammonium Persulfate
ATP	Adenosine Triphosphate
BH <sub>4</sub>	Tetrahydrobiopterin
CALCRL	Calcitonin receptor-like receptor gene
cAMP	Cyclic Adenosine Monophosphate
cDNA	Complementary DNA
cGMP	Cyclic Guanosine Monophosphate
CGRP	Calcitonin Gene-Related Peptide
CFH	Complement Factor H
CLR	Calcitonin receptor-Like Receptor
CRP	Complement Reactive Protein
DEPC	Diethyl Pyrocarbonate
DMEM	Dulbecco's Modified Eagle's Medium
DMSO	Dimethyl Sulfoxide
DNase	Deoxyribonuclease
dNTP	Deoxy-Nucleoside Triphosphate
dT	Deoxy-Thymine
EBSS	Earle's Balanced Salt Solution
ECL	Enhanced Chemiluminescence
EDTA	Ethylene-diamine-tetra-acetic acid
ELF	European Lead Factory
ELISA	Enzyme-Linked Immunosorbent Assay
EMEM	Eagle's Minimum Essential Medium
FBS	Foetal Bovine Serum
GAPDH	Glyceraldehyde 3-Phosphate Dehydrogenase
GPCR	G-Protein Coupled Receptor
GRK	GPCR kinase
HRP	Horse Radish Peroxidase
HUVEC	Human Umbilical Vein Endothelial Cell
IFN- $\gamma$	Interferon- $\gamma$
mA	Milliamps
MAOI	Monoamine oxidase inhibitor
MDD	Major Depressive Disorder
MTT	3-(4,5-dimethylthiazol-2-yl)-2,5-diphenyltetrazolium bromide
NO	Nitric oxide
PAGE	Polyacrylamide Gel Electrophoresis
PAM	Peptidylglycine alpha-Amidating Monooxygenase
PBS	Phosphate Buffered Saline
PEI	Polyethylenimine
PI3K	Phosphoinositide 3-Kinase

---

PIP3	Phosphatidylinositol (3,4,5)-trisphosphate
PVDF	Polyvinylidene Difluoride
RFU	Relative Fluorescence Units
RT-qPCR	Real-time Polymerase Chain Reaction
RAMP	Receptor Activity Modifying Protein
RIPA	Radio-immunoprecipitation assay
RPL13A	Ribosomal Protein L13A
RPMI	Roswell Park Memorial Institute
RT	Reverse transcriptase
SDS	Sodium Dodecyl Sulfate
SSRI	Selective serotonin reuptake inhibitor
TBS	Tris-buffered Saline
TCA	Tricyclic Antidepressant
TEMED	Tetramethylethylenediamine
TMB	3,3',5,5'-Tetramethylbenzidine

## Contents

1. Introduction	
1.1. Major Depressive Disorder	10
1.2. Adrenomedullin	11
1.3. FoxO3a	19
1.4. Project Aims	21
2. Materials and Methods	
2.1. Cell Culture	22
2.2. Quantitative Polymerase Chain Reaction	23
2.3. Adrenomedullin Receptor Antagonist Compounds	26
2.4. Cell Viability Assays	26
2.5. ELISAs	28
2.6. cAMP-Glo™ Max Assay	30
2.7. Western Blot	32
2.8. Transfection of ADM receptors in SH SY5Y cells	33
3. Results	
3.1. Gene Expression in Different Cell Lines	34
3.2. Cell Viability and Inflammation	35
3.3. Cyclic AMP Levels	37
3.4. Gene Expression in SK N SH Cells Treated with Antagonists and ADM	40
3.5. Western Blot	42
3.6. Transfection of ADM Receptors in SH SY5Y Cells	45
4. Discussion	
4.1. Cell Viability and Inflammation	45
4.2. Expression of the ADM Receptors	46
4.3. ADM-Mediated cAMP Production and the Effects Antagonist Pre-treatment	47
4.4. Gene Expression of Cells Treated with Antagonists	48
4.5. ADM-mediated FoxO3a Phosphorylation	49
4.6. Transfection of Cells with ADM Receptor Components	51
4.7. Conclusion	52



# 1. Introduction

## 1.1. Major Depressive Disorder

Major Depressive Disorder (MDD), also known as unipolar depression or major depression, is characterised as a negative mood (dysphoria) that lasts for more than two weeks at a time. The diagnosis of major depression may also require the presence of other physical or mental symptoms, including anhedonia (loss of pleasure in once pleasurable activities), persistent feelings of guilt and worthlessness, suicidal thoughts, weight loss (or in some cases weight gain), fatigue, inability to concentrate, and psychomotor retardation (Goodyer, 2003). It is one of the most common mental disorders in the world. In 2011, there was an estimated prevalence of 6.9 % of people in Europe (Wittchen et al., 2011), and this percentage is predicted to rise. This constitutes a large economic burden and current treatments for MDD have been shown to be ineffective and come with unpleasant side effects including nausea, headaches and sexual dysfunction (Ferguson, 2001).

NICE guidelines suggest that non-pharmacological treatments be attempted first, such as physical exercise and changes to the diet, as well as emotional support from friends and family. Anti-depressants are considered to be of low effectiveness relative to the risk they pose, especially in suicidal patients who may attempt to over-dose (NICE guideline, 2018).

The major classes of antidepressants currently used to treat MDD, along with other mood disorders, include tricyclic antidepressants (TCAs), monoamine oxidase inhibitors (MAOIs) and neurotransmitter reuptake inhibitors, such as selective serotonin reuptake inhibitors (SSRIs) (Herrman et al., 2009). These treatments are based on the monoamine hypothesis of major depression, the theory that depression is caused by the depletion of monoamine neurotransmitters in the central nervous system (Delgado, 2000). SSRIs are the first choice of anti-depressant, according to the BNF guidelines, due to the class being the most tolerated and safest drug when taken in over-dose. It is only when a patient fails to respond to SSRIs that other drugs, such as mirtazapine – an  $\alpha_2$ -adrenoreceptor antagonist, leading to increased noradrenergic and serotonergic neurotransmission – are prescribed (NICE, 2019). It is now believed that synaptic plasticity may be important in the pathology of depression in specific regions of the brain, including the hippocampus (Marsden, 2013). The number of patients who are non-responsive to anti-depressants is high, with varying reports on the actual percentage of non-responders to first line treatment. In 2004 a study investigating the treatment of MDD with SSRIs, found that 46% of patients did not respond (Corey-Lisle et al., 2004). As a result, there is a pressing need for new and more effective treatments for MDD to be developed.

Inflammation is thought to be of key importance in the pathology of depression. Increased childhood levels of inflammatory cytokines such as interleukin-6 (IL-6) and complement reactive protein (CRP), in children, are linked to an increased risk of developing depression. Cytokines are thought to promote dysregulation of the hypothalamic-pituitary adrenal (HPA) axis, also linked to depression (Kiecolt-Glaser et al., 2015). Treatments aimed at reducing inflammation and dysregulation of the HPA axis, in combination with SSRIs and other anti-depressants, may be the way forward for a more effective treatment for major depression.

### **1.1.1. Major Depressive Disorder and Adrenomedullin**

Patients with MDD were found to have elevated levels of adrenomedullin (ADM) and nitric oxide (NO) compared to healthy controls (Akpinar et al., 2013). The reason for this has yet to be elucidated, however Akpinar et al. suggested the neuroprotective role of ADM against inflammation and oxidative stress as a possibility. On the other hand, the elevated levels of ADM may be contributing to the pathology of MDD, potentially exacerbating the condition via the role of ADM in the regulation of the HPA axis.

ADM is thought to be involved in the regulation of the HPA axis, which is involved in the response to different types of stress. ADM and its receptor components, CLR and RAMP2, are expressed in the hypothalamus, pituitary gland and adrenal gland. ADM knockout in mice resulted in anxiety and other behavioural changes in response to stress. ADM administered to the pituitary gland, also led to decreased adrenocorticotrophic hormone (ACTH) secretion. ACTH is a hormone secreted in response to stress conditions. This suggests that ADM has a role in regulating response to stress via the HPA axis (García-Sanmartín et al., 2013). Hyperactivity of the HPA axis, due to reduced response to negative feedback mechanisms, has been linked to MDD and is thought to be involved in the predisposition of individuals to developing the disorder (Pariante & Lightman, 2008). Increased ADM levels in MDD patients may be in response to a hyperactive HPA axis.

There is evidence that ADM may play an important role in the response of individuals to anti-depressant treatment. A single-nucleotide polymorphism (SNP), resulting in altered *ADM* expression, affects the probability of MDD patients responding to the anti-depressant, paroxetine. Patients expressing the allele resulting in increased expression of the *ADM* were more likely to respond to treatment with paroxetine (Glubb et al., 2010). This further supports the role of ADM in MDD. Response to anti-depressant treatment has also been linked to inflammation and oxidative stress. Patients with higher levels of inflammation markers, tumour necrosis factor alpha (TNF- $\alpha$ ) and IL-6, and oxidative stress markers, 8-OH 2-deoxyguanosine (8-OHdG) and F2-isoprostanes, were less likely to respond to treatment with SSRIs (Lindqvist et al., 2017). Therefore, the antioxidant properties of ADM (Hu et al., 2017) may improve MDD patient response to anti-depressants. Therefore, although it is clear that ADM is important in MDD, it is unclear whether increased levels of ADM are beneficial or detrimental.

## **1.2. Adrenomedullin**

### **1.2.1. Physiology and Pathophysiology**

ADM is a vasodilator, peptide hormone and was first discovered in 1993 by Kitamura et al., from pheochromocytoma tissue extracts. Pheochromocytoma is a tumour of the adrenal medulla. ADM was so named as it was isolated from both healthy and pheochromocytoma tissue of the adrenal medulla (Kitamura et al., 1993). In addition to the adrenal medulla, ADM is also synthesised in almost all mammalian tissue types including endothelial cells, vascular smooth muscle cells and the central nervous system.

Since its discovery, ADM has been implicated in a range of different diseases including cancer, cardiovascular disease and neurological disorders (Ferrero et al., 2018a; Nishikimi et al., 2013; Qiao et al., 2017). Increased levels of ADM have been linked to decreased tubulin acetylation in Alzheimer's disease. This suggests ADM could have a role in cytoskeleton destabilisation and potentially neuronal plasticity (Ferrero et al., 2018b), which may be relevant in the role of ADM in MDD.

#### **1.2.1.1. Complement factor H**

Complement factor H (CFH) is a peptide involved in the alternative pathway of the complement system. It regulates this aspect of the immune system, helping to protect the body's healthy cells. In the blood plasma, ADM is bound by CFH which, as a result, is also known as adrenomedullin binding protein 1 (AMBP1) (Pio et al., 2001).

#### **1.2.2. Structure**

ADM is a member of the calcitonin peptide family, which also includes calcitonin, calcitonin gene-related peptide (CGRP), amylin and the most recently discovered, adrenomedullin 2 (ADM2), also known as intermedin. The peptides in this family share a similar simple secondary structure. However, ADM has an extended N-terminal region with 15 amino acids before the six amino acid ring structure, compared to just one amino acid for CGRP.

All of the peptides have an N-terminal ring structure, formed by a disulphide bond between two cysteine residues, and a C-terminal amidated aromatic residue. In ADM, the disulphide bond is formed between cysteine residues 16 and 21, and the amidated C-terminal residue is tyrosine. Receptor binding experiments have shown that amidation of the C-terminal residue is essential for receptor binding and the N-terminal ring structure is essential for activation of the receptor (Robinson et al., 2009). Figure 1.1 shows the primary structure of the mature ADM peptide and highlights the disulphide bond forming the N-terminal ring, as well as the amidated C-terminal tyrosine.

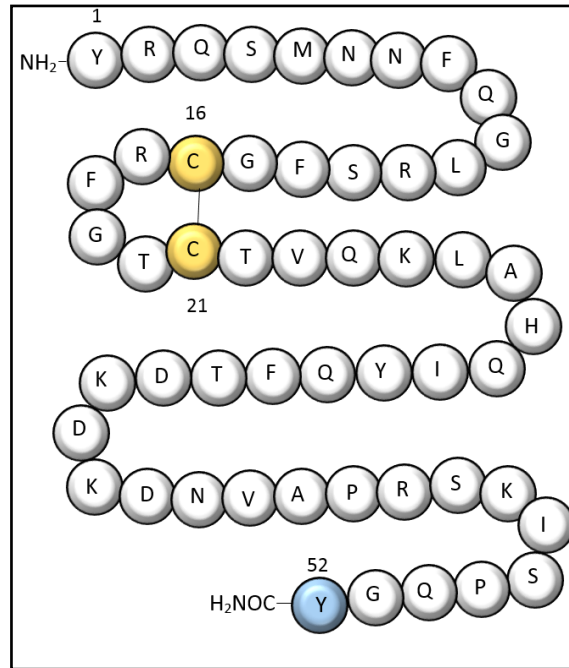


Figure 1.1. The structure of the mature ADM peptide

The structure reveals the six-amino acid ring structure, formed by a disulphide bond between Cys 16 and 21, and the amidated c-terminal Tyr 52. Cys 16 and 21 are shown in yellow, and Tyr 52 is shown in blue.

Although the members of the calcitonin peptide family share the essential structural features required for receptor binding and activation, the peptides share little of their amino acid sequences. Figure 1.2 shows the sequence alignment of human ADM, ADM-2 and CGRP. The residues highlighted in green are the only identical amino acids shared across all three of the peptides. As the names suggest ADM shares the highest sequence identity with, and is therefore likely to be most closely related to, ADM2 at 34 % identity, whereas between ADM and CGRP sequence identity is just 19 %.

	10	20	30	40	50
ADM1c1 Query_10001	YRQSMNNFQGLRSFG	REFGTC	TVQKLAHQIYQFTD	-KDKDNVAPRSKI	SPQGY
AM21c1 Query_10002	-----TQAQLLRVGV	LVLGTC	QVQNL	SHRLWQLMGPAGRQDSA	FVDPSSPHSY
CGR1c1 Query_10003	-----ACDTAT	CVTHRI	LAGLLSRSGG	-VVKNNFVPTNVG	SKAF-

Figure 1.2. ADM vs ADM2 vs CGRP human peptide sequence alignment

The alignment was made using the U.S. National Library of Medicine's Constraint-based Multiple Alignment Tool (COBALT) – [www.ncbi.nlm.nih.gov/tools/cobalt/re\\_cobalt.cgi](http://www.ncbi.nlm.nih.gov/tools/cobalt/re_cobalt.cgi). Top line = Adrenomedullin, middle line = Adrenomedullin 2 and bottom line = Calcitonin Gene-Related Peptide. Green highlighted residues = residue identity between peptide sequences. Grey highlighted residues = residues with similar properties.

### 1.2.3. ADM gene and peptide processing

The gene encoding ADM was first discovered and sequenced in 1994 (Ishimitsu et al., 1994). *ADM* is located on chromosome 11 in humans, and is made up of four exons and three introns. The gene

actually codes for a 185 amino acid precursor protein known as preproadrenomedullin (preproADM) (Beltowski & Jamroz, 2004). The start codon for preproADM is located in exon 2 and the sequence coding for the mature ADM peptide is located entirely in exon 4 (Ishimitsu et al., 1994).

Proteolytic cleavage of preproADM yields proadrenomedullin N-terminal 20 peptide (PAMP) and ADM, both are biologically active. The precursor peptide is initially cleavage at the site between Thr21 and Ala22, removing the N-terminal signal sequence and leaving a 164 amino acid propeptide, proadrenomedullin (proADM)(Dipette & Supowit, 2008). ProADM is cleaved at the site Lys43-Arg44, producing the PAMP peptide, which is C-terminal amidated to form the active peptide. Mature ADM is formed from residues 95-146 of the preproADM precursor peptide (Beltowski & Jamroz, 2004; Dipette & Supowit, 2008). The glycine residue 147 is included in the immature ADM peptide and is processed by the peptidylglycine alpha-amidating monooxygenase (PAM) enzyme, forming the amidated C-terminal tyrosine of the mature ADM peptide. Figure 1.3. shows which amino acids of the precursor peptide form the biologically active peptides, PAMP and ADM.

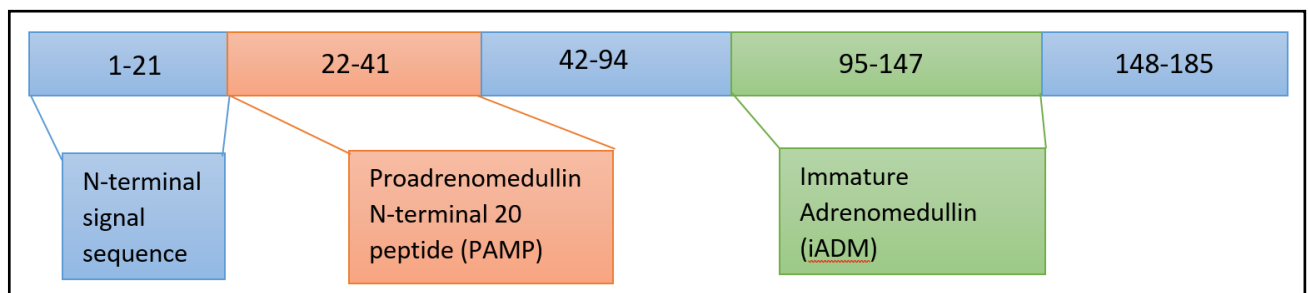


Figure 1.3. The precursor peptide of ADM, preproADM, encoded by *ADM*

The N-terminal signal sequence is cleaved and amino acids 95-147 produce the immature form of Adrenomedullin (iADM), with amino acids 22-41 forming the other biologically active peptide coded for by *ADM*, PAMP. Immature ADM is further processed by the enzyme peptidylglycine alpha-amidating monooxygenase (PAM), forming the amidated Tyr from the C-terminal glycine residue.

#### 1.2.4. Receptors

The ADM receptors are formed from two proteins, the calcitonin receptor-like receptor (CLR) and a receptor activity modifying protein (RAMP), either RAMP 2 or RAMP 3. The CLR is a G-protein coupled receptor (GPCR), belonging to the class B family of GPCRs and its structure is similar to the other GPCRs in this class. It comprises of a seven-transmembrane domain (7 TMD) and a large N-terminal extracellular domain (ECD) (de Graaf et al., 2017). Peptide ligands bind to class B GPCRs in a manner known as the 'two domain model' where the C-terminus of the peptide binds to the ECD of the receptor and the N-terminus binds to the TMD, activating the receptor (Parthier et al, 2009). This model explains the importance of the C-terminal amidated tyrosine residue for the binding of the ADM peptide to the ADM receptors, and the requirement of the N-terminal ring structure, formed by the disulphide bond, for ADM-mediated activity.

There are three known RAMPs, namely RAMP 1, 2 and 3. Human RAMPs 1 and 3 have a precursor protein length of 148 amino acids whereas RAMP 2 is larger with a precursor length of 180 amino acids. They share little sequence identity but have a similar basic structure consisting of a large extracellular domain, single transmembrane domain and a short cytoplasmic domain (Sexton et al.,

2001). RAMPs have two functional roles in the ADM receptors. One role involves facilitating the trafficking of the CLR from the endoplasmic reticulum (ER), through the Golgi body, to the cell surface membrane (McLatchie et al., 1998). A reason for this might be that RAMP binding to CLR stabilises the structure of the receptor, allowing proper folding of the protein and therefore allowing CLR to exit the ER. Without the expression of a RAMP, the CLR is not glycosylated at the N-terminus, a requirement for receptor processing, and remains in the ER of the cell (Bolander Jr, 2004; Dickenson et al., 2013). The transport pathway of CLR to the cell surface is shown in Figure 1.4. RAMPs also determine the pharmacology of the receptor. CLR/RAMP2 forms the ADM<sub>1</sub> receptor and CLR/RAMP3 forms the ADM<sub>2</sub> receptor, both are specific for ADM, however CLR/RAMP1 forms a receptor specific to CGRP. Figure 1.5 shows the basic structure of the ADM receptors. It is worth noting that there is some cross specificity for ADM and CGRP between these receptors, with ADM<sub>2</sub> and CGRP receptors activated by both ADM and CGRP, yet ADM<sub>1</sub> is highly specific for ADM (Hay et al., 2004). The selectivity of the receptors is determined by the RAMP, via allosteric interactions with the CLR component of the receptor and direct interactions with residues of the peptide ligand. An example of an important interaction between a RAMP and the peptide ligand is the hydrogen bonding of RAMP2 residue E101 with the ADM terminal residue Y52, discovered via X-crystallography structure determination of the ECD domain of RAMP2:CLR (Booe et al., 2015; Booe et al., 2018).

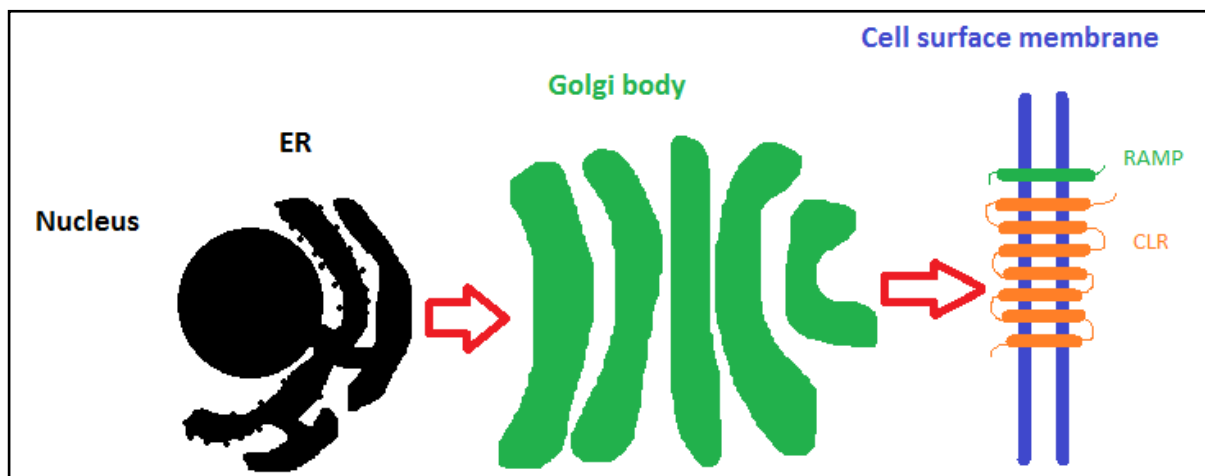


Figure 1.4. Representation of the pathway of the receptor from the ER to the cell surface membrane. The RAMP is essential for the movement of the CLR receptor component to the cell surface. The reason for this may be that the RAMP aids the proper folding of the CLR, as it is vital that a protein is properly folded before it can exit the ER.

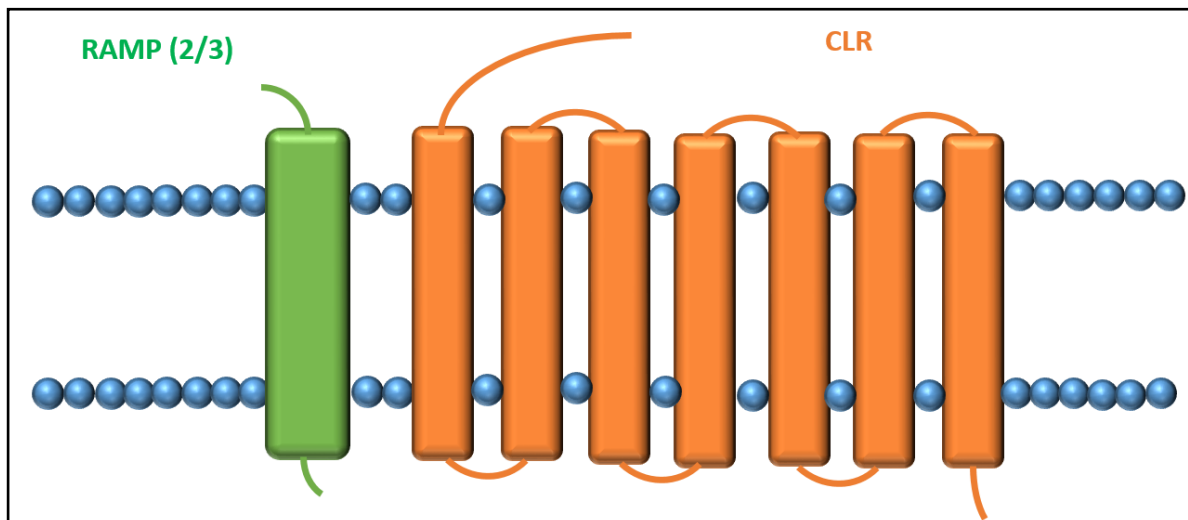


Figure 1.5. Representation of the ADM receptor  
 The CLR component of the receptor has seven transmembrane domains and the accompanying RAMP has a single transmembrane domain.

### 1.2.5. Current understanding of signalling pathways

The majority of the literature on ADM-mediated signalling is focussed on cAMP production via adenylate cyclase activation and initially this was thought to be the only pathway activated upon ADM binding to its specific receptors (Hay et al., 2018; Yoshimoto & Hirata, 2005). This is not surprising as the peptide was discovered due to its ability to elevate cAMP levels in platelets (Kitamura et al., 1993). However, it has since been elucidated that multiple other signalling pathways are involved in mediating the physiological effects of ADM including the NO/cGMP, PI3K/Akt and ERK/MAPK pathways (Yoshimoto & Hirata, 2005).

Studies have shown that certain physiological effects of ADM, including inhibition of apoptosis and vasodilation, are mediated by the activation of the NO/cGMP pathway (Matteo & May, 2003; Sata et al., 2000). The activation of the ADM receptor stimulates neuronal nitric oxide synthase (nNOS) to produce nitric oxide (NO) which, in turn, stimulates guanylate cyclase (GC) to produce cGMP. A summary of the canonical ADM signalling pathway and how this leads to NO and cGMP production is shown in Figure 1.6.

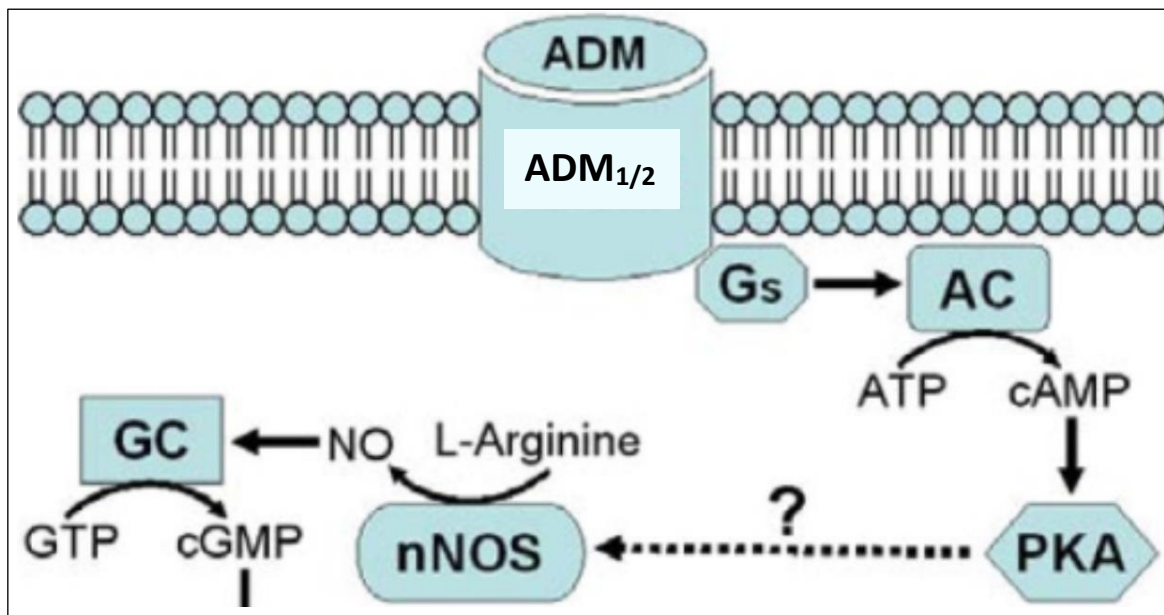


Figure 1.6. Canonical signalling pathway of ADM and mechanism for ADM-mediated NO production adapted from Figure 7 of (Yen et al., 2011)

ADM binding to the receptor activates the G protein bound to the CLR component of the receptor. The G<sub>as</sub> subunit of the G protein activates adenylate cyclase, stimulating the production of cAMP. Neuronal NOS is activated via PKA, stimulating NO production, which activates guanylate cyclase to produce cGMP.

The main component of the ADM receptors and the CGRP receptor is the CLR, which is a class B GPCR. The signalling pathway activated by a GPCR is determined by the G-protein. The activation of adenylate cyclase (AC) is mediated by the coupling of the ADM receptor to the G<sub>α<sub>s</sub></sub> protein. This leads to the inhibition of cAMP production by AC. As ADM stimulation mainly leads to the production of cAMP, it is thought that the ADM receptor is primarily coupled to the G<sub>α<sub>s</sub></sub> protein.

The CGRP receptor is also suggested to interact with the G<sub>α<sub>s</sub></sub> protein as well as the G<sub>α<sub>q/11</sub></sub> protein and also mediate G-protein independent signalling, via β-arrestin (Walker et al., 2016). Studies investigating ADM and CGRP receptor-binding activity have also suggested that some of the physiological effects of ADM may be mediated via the CGRP receptor. Therefore pathways activated by these G-proteins may also be relevant to ADM activity (Yoshimoto & Hirata, 2005). The ADM receptors could also activate these pathways.

Beta-arrestins are adaptor proteins that are involved in GPCR signalling desensitization. The conformational change caused by receptor-ligand binding results in recognition by GPCR kinases (GRKs). GRK 4 and 5 recognise the ADM receptors (Kuwasako et al., 2016), which phosphorylate the C-terminal of the receptor specific sites. These sites are recognised by β-arrestins and the receptor is internalised, preventing further activation of G-protein-mediated signalling (Kovacs et al., 2009).

Initially β-arrestins were thought to only be involved in receptor desensitisation, however the adaptor proteins are now associated with the activation of signalling pathways including the PI3K/Akt pathway. The mechanisms by which β-arrestins interact with these pathways are complex and can inhibit or activate the signalling molecules depending on the proteins recruited by the β-arrestin (DeFea, 2008). β-arrestin 1 was found to activate PI3K, leading to the subsequent phosphorylation and activation of Akt in insulin growth factor 1 (IGF-1) signalling (Povsic et al.,

2003). ADM has been found to activate the PI3K/Akt pathway to inhibit apoptosis, as with IGF-1 signalling, and due to the association with ADM/CGRP receptors and  $\beta$ -arrestin mediated signalling, potentially ADM could activate PI3K/Akt signalling via this mechanism (Povsic et al., 2003).

PI3K can also be activated by the  $G_{\beta\gamma}$  complex, a dimeric complex which binds to the  $G_{\alpha}$  subunit of the G protein complex when the GPCR is inactive, releasing the subunit upon ligand binding and GPCR activation (Schwindinger & Robishaw, 2001; Stephens et al., 1994). Therefore, there is also a possibility that ADM could activate the PI3K/Akt pathway via this mechanism.

### 1.2.6. CGRP-receptor component protein (RCP)

Another component of the ADM receptors, suggested to be important for signal transduction, is the CGRP-receptor component protein (RCP). In humans CGRP-RCP is 148 amino acids in length. The protein is highly conserved across species with the human, mouse and rat forms of the protein sharing almost 90 % sequence identity.

RCP has been found to interact directly with the CLR component of the ADM and CGRP receptors and enhance the ADM/CGRP-mediated signal. However, RCP does not affect the affinity of the ligand for the receptor (Evans et al., 2000). RCP is expressed in most immortalised cell lines, yet *in vivo* expression is more specific to cell subsets (Dickerson, 2013). RCP expression localises to CGRP-responsive sites (Rosenblatt et al., 2000).

There is much evidence that RCP is important in enhancing ADM and CGRP receptor activity when  $G_{\alpha s}$  is coupled to the receptor leading to an increase in intracellular cAMP levels. However, it is yet to be made clear whether RCP is important in other signalling pathways mediated by ADM. It may be that RCP is involved in signalling biased, resulting in the observed favouring of the cAMP signal pathway. *In vivo*, cells, which do not express RCP, may mediate the physiological effects of ADM via alternative pathways, such as the PI3K/Akt pathway.

### 1.2.7. Peptide antagonists and Adrenomedullin Modulators

All of the current ADM antagonists are peptide-based. These are truncated versions of ADM without the N-terminal ring structure. One such fragment is ADM<sub>22-52</sub>, which is the only commercially available antagonist. However, ADM<sub>22-52</sub> has low affinity for the receptors. Robinson et al. developed other peptide antagonists of the CGRP and ADM receptors, by experimenting with different peptide truncations and peptide chimeras of ADM and  $\alpha$ CGRP. They demonstrated regions of the peptides required for determining the receptor specificity and also residues that may be involved in interactions with the RAMP components of the receptor, however were unable to develop an antagonist significantly more effective than the existing ADM<sub>22-52</sub> (Robinson et al., 2009).

Despite the availability and effectiveness of ADM<sub>22-52</sub> at inhibiting the ADM receptors, the development of a small molecular antagonist is desirable. This is because, peptide-based therapeutics are often unstable due to the oral unavailability and short plasma half-life of peptides. This is particularly relevant in regards to ADM which has a half-life of only around 22 minutes (Meeran et al., 1997). A small molecular antagonist would allow the progression of research on the

different signalling pathways the receptors may activate and would have the potential to be developed into a clinical treatment for the multiple ADM-associated diseases.

Martínez et al. screened small molecules that were able to modulate the effectiveness of ADM, positively or negatively (Martínez et al., 2004). The compounds were initially screened for their ability to block the interaction of the ADM peptide and an anti-ADM, neutralizing monoclonal antibody. The compounds were then evaluated on the effect they had on cAMP levels when administered to cells also treated with ADM. Some of the compounds were able to reduce the level of cAMP, compared to ADM alone, whereas others increased the level of cAMP (Martínez et al., 2004). Although these small molecules appear to disrupt or enhance ADM signalling, and experiments using these small molecules suggest that they can affect ADM-associated effects related to cancer (Ochoa-Callejero et al., 2017; Siclari et al., 2014), the mechanism of how they achieve these effects is unclear. Martínez et al. suggest that the small molecular modulators act by binding to ADM itself (Martínez et al., 2004), rather than the receptors, and therefore may be effective through causing a conformational change of ADM rather than binding to its receptors.

### 1.3. FoxO3a

ADM signalling is not only mediated via adenylate cyclase activation and cAMP, but also via PI3K and Akt activation (Miyashita et al., 2003). Phosphorylation of FoxO3a by Akt blocks the transcriptional activity of the protein and reduced levels of FoxO3a has been shown to have more long-term neuroprotective effects (Sun et al., 2018). Therefore, perhaps the neuroprotective effects of ADM are mediated by the Akt-phosphorylation and inhibition of FoxO3a.

Forkhead box-containing (FoxO) proteins are a subgroup of transcription factors. The nematode homolog is known as Daf-16 and is involved in determining lifespan (Kenyon et al., 1993). There are also four mammalian FoxOs: FoxO1, FoxO3 (FoxO3a), FoxO4 and FoxO6, and a fruit fly (*Drosophila melanogaster*) homolog dFoxO (McLaughlin & Broihier, 2018).

The nuclear localisation of the forkhead-box transcription factor FoxO3a results in cell apoptosis. Treatment of PC12 cells with corticosterone mimics the hyperactivity of the HPA axis, which has been linked to mood disorders such as anxiety, depression and schizophrenia (Bradley & Dinan, 2010; Varghese & Brown, 2001), and leads to cell apoptosis. Clozapine is an antipsychotic drug used to treat refractory schizophrenic patients and was found to inhibit corticosterone-induced apoptosis, via the PI3K/Akt/FoxO3a pathway. Treatment of cells with clozapine increases the phosphorylation of Akt and FoxO3a, which inactivates the transcription factor and prevents its translocation into the nucleus (Zeng et al., 2017). This suggests activation of PI3K/Akt, and therefore inactivation of FoxO3a, could be neuroprotective. ADM has been shown to prevent apoptosis in cardiomyocytes via activation of the PI3K/Akt pathway (Okumura et al., 2004). Perhaps this mechanism of action in cardiomyocytes is dependent on FoxO3a. Our hypothesis is that ADM may be able to inhibit FoxO3a transcriptional activity, via PI3K/Akt –dependent phosphorylation. This may occur by ADM binding to its receptor and activating the G protein bound to the receptor. The G protein then separates into the  $G_{\alpha s}$  component, which activates adenylate cyclase, and the  $G_{\beta\gamma}$  component, which is thought to activate PI3K (Merlot & Firtel, 2003). Akt (also known as protein kinase B) is then activated via the PI3K-dependent phosphorylation of PIP2 to form PIP3, which activates PDK1 and, in turn, Akt. Akt phosphorylates FoxO3a at the sites Thr 32, Ser 253 and Ser 315 (Tzivion et al., 2011). FoxO3a in its phosphorylated form is unable to translocate across the nuclear membrane and, as a result, is no

longer transcriptionally active. A summary of the proposed pathway of ADM-mediated inhibition of FoxO3a transcriptional activity is shown in Figure 1.7.

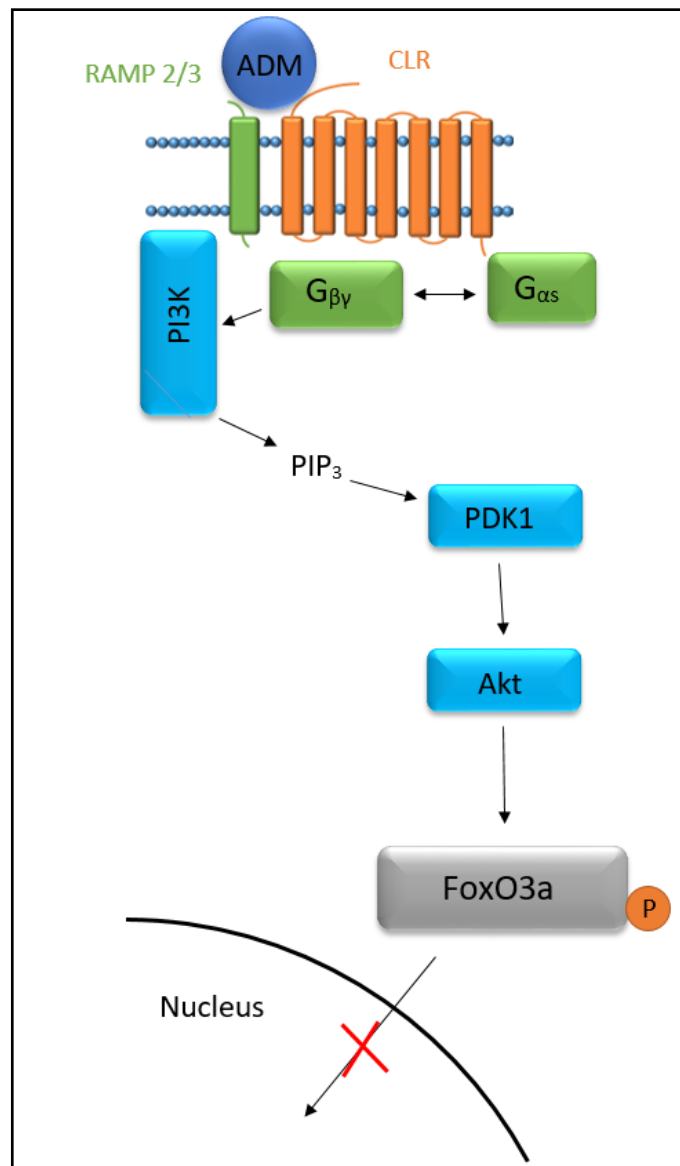


Figure 1.7. The possible mechanism by which ADM could mediate the inhibition of the Foxo3a transcription factor

Analysis of RNA polymerase II activity in coding regions, rather than measuring mRNA levels, has revealed that FOXO3 transcriptionally regulates a variety of genes. These include, but are not limited to, genes involved in the PI3K/Akt signaling pathway (*IGF1R*, *IRS2* and *RICTOR*) and in the cell-cycle (*CCNB1* and *CCNG2*) (Eijkelenboom et al., 2013). *IGF1R* and *IRS2* code for insulin-like growth factor receptor 1 and insulin receptor substrate 2, respectively, and have been linked to longevity via the inhibition of FoxO3a via the PI3K/Akt pathway. *RICTOR* codes for a protein which is part of the mTOR complex 2, involved in Akt-dependent FOXO phosphorylation. *IGF1R*, *IRS2* and *RICTOR* are all down regulated by FoxO3a, suggesting a mechanism of auto negative regulatory feedback (Eijkelenboom et al., 2013). *CCNB1* and *CCNG2* code for cyclins B1 and G2, respectively. These cyclins are involved in the regulation of the cell-cycle. Cyclin B1 promotes the cell to leave the G2 phase of the cell cycle and enter mitosis, and so promotes cell-cycle progression and cell proliferation. Cyclin G2 is an atypical cyclin that inhibits cell-cycle progression. FoxO3a was found to down regulate *CCNB1* and up

regulate *CCNG2* (Eijkelenboom et al., 2013). This suggests FoxO3a prevents cell proliferation. Therefore, if ADM inhibits FoxO3a, this could partially explain increased levels of ADM in cancer patients (Larráyoz et al., 2014).

## 1.4. Project Aims and Objectives

There are many individuals who do not respond to available antidepressant treatments, and those who do respond still have to face the possibility of unpleasant side effects. Therefore, there is a demand for a new, more effective therapeutic to be developed, to treat or increase the effectiveness of current treatments for MDD, and reduce side effects. ADM has been shown to be increased in patients with MDD (Akpınar et al., 2013; Mahajan et al., 2017) and as a result is a potential target for the development of a therapeutic to treat the disorder. However, currently, there are no known small molecular ADM receptor antagonists available.

Seven small molecules have been identified via high-throughput screening of the European Lead Factory's (ELF) compound library. These molecules are possible antagonists of the ADM<sub>2</sub> receptor. The aim of this project was to assess the ability of the compounds to antagonise ADM activity in cell lines where the ADM receptors are naturally expressed, whereas in the ELF assays the receptors were stably transfected into the cell line, and to ensure the ELF results could be recapitulated. Although ELF have only selected for compounds against the ADM<sub>2</sub> receptor, we also assessed the ability of the compounds to antagonise the ADM<sub>1</sub> receptor. This is because there is known cross-specificity for ligands of the two receptors (Weston et al., 2016) and so the antagonists may bind to and be active against both of the receptors.

The ELF initial testing only assessed the ability of the compounds to inhibit ADM-mediated cAMP level increase; therefore, another aim of the project was to investigate whether the compounds could affect other signalling pathways induced by ADM. The pathway chosen for this was the PI3K/Akt signalling pathway, specifically the effect of activated Akt-mediated phosphorylation of FoxO3a.

The hypothesis of the project is that the small molecule ADM receptor antagonists will be able to block ADM-mediated signalling via cAMP and via PI3K/Akt dependent phosphorylation of FoxO3a.

In summary, the main objectives of this project were as follows:

- Identify suitable cell lines to investigate the effects of the ADM receptor antagonists
- Use pathways known to be involved in ADM signalling (cAMP) to verify the ability of the antagonists to inhibit ADM-mediated activity
- Investigate other pathways that may be involved in ADM activity (PI3K/Akt dependent FoxO3a phosphorylation) and the effects of the antagonist compounds on these pathways

## 2. Materials and Methods

### 2.1. Cell Culture

During culture, cells were incubated in standard conditions of 21 % oxygen, 5 % carbon dioxide and at a temperature of 37 °C, unless otherwise stated. The cell lines THP-1, SH SY5Y, 1321N1 and SKNSH were purchased from the European Collection of Authenticated Cell Cultures (ECACC). Human umbilical vein endothelial cells (HUVECs) were supplied by ATCC.

### **2.1.1. THP-1 Cells**

THP-1 cells are a monocytic cell line derived from a patient with acute monocytic leukaemia. As this cell line is haematopoietic, the cells grow in suspension. As a result, the passaging of the cells involved removing half of the cells from the flask and topping up the volume in the flask with fresh media. Media requirements for the THP-1 cells were as follows: RPMI 1640 Medium (SigmaAldrich, Missouri, USA) + 10% FBS+ 2mM L-glutamine.

### **2.1.2. SH SY5Y Cells**

SH SY5Y cells are a neuroblastoma cell line, which are a subclone of the SK N SH cell line. SK N SH cells were originally isolated from the bone marrow of a four-year old female patient with neuroblastoma. The cell line is adherent and forms a monolayer in the cell culture flask. To passage the cells, the medium was removed and the cells were washed with PBS. The PBS was removed and 1x trypsin was added to the layer of cells, at a ratio of approximately 40-100 µL per 1 cm<sup>2</sup> of surface area. The cells were incubated for 4 minutes at 37 °C. Fresh medium was added to the cells at twice the volume of trypsin added. The cells were vigorously agitated to ensure all cells were detached from the flask and to create a single cell solution. The cells were centrifuged at 500 x g for 5 mins, to remove the trypsin. The supernatant was removed and the cell pellet was resuspended in fresh medium. Cells were split 1:8 with medium and placed back in incubation at 37 °C, in a humid environment. Cells were allowed to reach 70-80 % confluency before passaging, with a maximum passage number of 20. The medium requirements for SH SY5Y cells were as follows: Ham's F12:EMEM (Gibco, Dublin, Ireland) (EBSS) (1:1) + 2 mM L-glutamine + 10 % Foetal Bovine Serum (FBS).

### **2.1.3. Astrocytes – 1321N1 cell line**

The astrocytes grown for this project were human and of the 1321N1 cell line. As the name suggests, the astrocytes were derived from human astrocytoma tissue. The cells have a short doubling time and required passaging every couple of days. They are an adherent cell line and are passaged in the same way as SH SY5Y cells. The media requirements for these astrocytes were DMEM (SigmaAldrich, Missouri, USA) + 2 mM L-glutamine + 10 % FBS.

### **2.1.4. Human Umbilical Vein Endothelial Cells (HUVECs)**

HUVECs are primary cells isolated from the vein of human umbilical cords. HUVECs may be derived from multiple donors and also from donors of different ethnic backgrounds. Therefore, the cells may

differ on a genetic and molecular level, and so it is important to consider these factors when using the cells in experiments (Nor Suhaila & Safuan, 2017). The cells were passaged and maintained in the same way as SH SY5Y cells in section 2.1.2. HUVECs appeared to grow at slower rate than that of SH SY5Y cells however and so required passaging less frequently. In addition, HUVECs can only reach a passage number of between 5 and 10 before becoming non-viable. The cells were grown in Endothelial Cell Growth Medium (Cell Applications inc., California, USA.) which was supplied already containing serum and growth factors.

### **2.1.5. SK N SH**

As mentioned in section 2.1.2., SK N SH cells were originally derived from metastatic neuroblastoma tissue in the bone marrow of a four-year old female. SK N SH is a neuronal cell line and contains a high level of dopamine- $\beta$ -hydroxylase, usually found in the sympathetic nervous system (Biedler et al., 1973). This cell line has a relatively long doubling time, making them difficult to grow up to a large scale. SK N SH are an adherent cell line and so were passaged in the same way as SH SY5Y cells and HUVECs. The cells adhere quite sensitively and so, for assays where numerous washing and medium changes occurred, the cells were grown on cell culture plates with the Cell<sup>+</sup> growth surface (Sarstedt, Nümbrecht, Germany). The medium requirements for this cell line were DMEM (SigmaAldrich, Missouri, USA) with 2 mM L-glutamine and 10 % FBS.

## **2.2. Real Time Quantitative Polymerase Chain Reaction (RT-qPCR)**

### **2.2.1. Sample preparation for the gene analysis of cells treated with antagonists and ADM**

To analyse the gene expression in SK N SH cells after treatment with antagonists and ADM, cells were plated out at a density of  $5 \times 10^5$  cells per well of a 6 well plate with the Cell<sup>+</sup> growth surface (Sarstedt, Nümbrecht, Germany). The cells were incubated at 37 °C for 48 hours. The medium was aspirated and the cells were washed with PBS before the medium was replaced with serum-free DMEM. Cells were pre-treated with 10  $\mu$ M of antagonist and incubated at 37 °C for 30 minutes. The cells were then treated with 0.1  $\mu$ M of ADM<sub>13-52</sub> agonist (GenScript, New Jersey, USA) and incubated for 6 hours at 37 °C. RNA extraction was performed as standard. ADM<sub>13-52</sub> acts as an agonist of the adrenomedullin receptors and was used due to the degradation of the full ADM peptide. DMSO was added to the same concentration as for the samples treated with the antagonist compounds.

### **2.2.2. RNA Extraction**

The medium was aspirated and the cells were washed using PBS. One mL of TRIzol reagent (Invitrogen) per 10 cm<sup>2</sup> was added to each well. The cells were scraped in the TRIzol and the solution was made homogenous using a micropipette. Chloroform was added to the cells at a ratio of 0.2 mL

per 1 mL of TRIzol, the sample was shaken vigorously and incubated at room temperature for 2-15 minutes. After incubation, the samples were centrifuged at 12,000 x g for 15 minutes.

The samples were separated into three phases containing protein, DNA or RNA. The upper colourless aqueous phase contained RNA. This phase was collected and transferred to a tube containing isopropanol at a ratio of 0.5 mL to 1 mL of TRIzol used during cell lysis. The sample was incubated at room temperature for 5-10 minutes and then centrifuged at 12,000 x g for 10 minutes. The supernatant was removed and the RNA pellet was resuspended, using 75 % ethanol at a ratio of 1 mL per 1 mL of TRIzol initially used. The sample was vortexed and centrifuged at 7,500 x g for 5 minutes. The supernatant was removed and the RNA pellet was air-dried for 5-10 minutes. Thirty to fifty microliters of DEPC-treated TE (Tris-EDTA) buffer was added, with the volume depending on the pellet size, and the sample was mixed by micro pipetting. The sample was placed in a heat block at 55-65 °C for 10-15 minutes.

The quality of the extracted RNA was then analysed using nanodrop, measuring the  $A_{260}/A_{280}$  ratio to check the purity of the RNA. The  $A_{260}/A_{280}$  ratio for pure RNA is around 2.0 however, a ratio of around 1.8 is acceptable. The RNA was also analysed using 1 % agarose gel electrophoresis, in order to identify any presence of genomic DNA or degraded RNA.

### 2.2.3. cDNA Synthesis

The extracted RNA was treated with DNase, to degrade the genomic DNA in the sample. This ensures the primers, used in the PCR reactions, do not amplify gene sequences from genomic DNA and only amplify cDNA sequences. DNase was added to the RNA at a ratio of 0.5  $\mu$ L to 4  $\mu$ L sample, containing a maximum of 500 ng of RNA, along with 0.5  $\mu$ L DNase buffer was added, giving a total volume of 5  $\mu$ L. The concentration of DNase I used was between 50-375 units/ $\mu$ L according to the supplier (Invitrogen, California, USA).

The sample was gently micro-centrifuged and incubated at 37 °C for 60 minutes. 0.5  $\mu$ L 0.5 M EDTA was added and the sample was gently micro-centrifuged. In order to denature the DNase enzyme, the sample was incubated at 65 °C for 10 minutes.

For the cDNA synthesis reaction, a master mix of: 2  $\mu$ L cDNA synthesis buffer, 1  $\mu$ L dNTPs, 0.5  $\mu$ L random hexamers, 0.5  $\mu$ L Oligo dTs and 0.5  $\mu$ L reverse transcriptase enzyme (Verso enzyme mix) was prepared. In the RT- controls, nuclease free water was added in place of the reverse transcriptase. Four  $\mu$ L master mix was added to each RNA sample. The samples were incubated at 42 °C for 60 minutes and then incubated at 95 °C for 2 minutes. The samples were diluted with nuclease free water, to give a 1:5 stock dilution.

### 2.2.4. Quantitative Polymerase Chain Reaction (RT-qPCR)

The genes investigated using RT-qPCR were *ADM* (adrenomedullin), *RAMP1* (receptor activity modifying protein 1), *RAMP2*, *RAMP3*, *CALCRL* (calcitonin receptor-like receptor), *CALCA* (calcitonin gene-related peptide 1) and *CFH* (complement factor H). Real time quantitative PCR to analyse the relative expression of each of the genes in the different cell lines. All of the cell lines were human and therefore primers were designed for the human forms of the genes. The primers were designed

to be exon-exon spanning so that the primers would only bind to the cDNA of the gene of interest and not to full gene sequence of the genomic DNA. The sequences of these primers are given in table 2.1, and are presented in the 5' to 3' direction. A housekeeping gene, known to be stably expressed in a cell line, was used as a reference gene to normalise expression. The reference gene used was *GAPDH*. *GAPDH* codes for glyceraldehyde 3-phosphate dehydrogenase, an enzyme involved in glycolysis. The primers for the reference gene were purchased as a primer mix (containing both the forward and reverse primer) as part of a geNorm kit (Primerdesign Ltd., Southampton, UK). GeNorm analysis had previously been used to determine that *GAPDH* was stably expressed in the cell lines used. The gene is one of ten commonly used reference genes (Vandesompele et al., 2002).

For RT-qPCR, the cDNA being analysed was diluted, with nuclease free water, to give a final dilution of 1:50. The forward and reverse primers for the target genes of interest were diluted in nuclease free water to give a dilution of 1:5. A master mix of nuclease free water, forward primer, reverse primer and polymerase-nucleosides master mix (iTAQ) was prepared, at a ratio of 1.4 µL: 0.3µL: 0.3 µL: 3 µL per well, respectively, for each different gene. Five µL master mix was added to each well the RT-qPCR plate, along with 5 µL cDNA. The plate was centrifuged to mix.

The RT-qPCR reaction was performed using the CFX96 Touch™ Real-Time PCR Detection System (Bio Rad, California, USA). The parameters used for the qPCR reactions were as follows: 30 seconds at 95 °C to denature the DNA and activate the polymerase, 40 amplification cycles of 5 seconds at 95 °C followed by 30 seconds at the annealing temperature of 60 °C, finally melt-curve analysis was performed at 95 °C.

Table 2.1. Sequences of the primers used for real time PCR (RT-qPCR).

Gene	Primer direction	Sequence
CALCRL	Forward	GCTCTGCCCTGATTACTTTCA
CALCRL	Reverse	TCTGTTGCTTGCTGGATGTC
RAMP1	Forward	CCCATCACCTCTTCATGACCA
RAMP1	Reverse	CGACGGCCTCCATGTCTAC
RAMP2	Forward	CGCTGTCCTGAATCCCCA
RAMP2	Reverse	GCTGTCTCATAGTTCTTCACCG
RAMP3	Forward	CATGATGGGCAAGGTGGAC
RAMP3	Reverse	CCATCTCGGTGCAGTTGG
ADM	Forward	CCAGAGCATGAACAACCTCCA
ADM	Reverse	CGACGTTGTCCTTGTCTTA
CALCA	Forward	CAGGAGCAAGAGAGAGAGGG
CALCA	Reverse	AGCCGATGAGTCACACAGG
CFH	Forward	GGATACCTGCTCCGAGATGT
CFH	Reverse	CAGCTACTGGAAAGTATGGTCT

Notes: The Homo sapiens (human) genes are denoted using the standard nomenclature of all capital letters, e.g. CALCRL. The primer sequences used for each gene are shown. Sequences are presented in the 5' to 3' direction.

## 2.3. Adrenomedullin Receptor-Antagonist Compounds

The ELF delivered seven of the compounds found to be antagonists of the ADM<sub>2</sub> receptor to Huddersfield. The compounds and their assigned numbers are listed in Table 2.2. Some of the compounds are analogues of other compounds tested during the high throughput screening. The parent/analogue relationships of the compounds are described in Table 2.2. Each compound arrived in lyophilized, powder form and was dissolved in DMSO to produce a 10 mM stock solution. The stock solutions were stored at -20 °C. All compounds, except for 06 and 04, were white in powder form or colourless and clear when in solution. Compounds 06 and 04 were yellow-orange in colour when both in powder form and in solution. Compound 08 also developed a yellow tinge in solution over time; this may be potentially due to hydrolysis of the compound in storage. The structures of the compounds cannot be revealed due to a confidentiality agreement with the ELF.

Table 2.2. The ADM-receptor antagonist compounds

Antagonist Compound	Huddersfield Vial Number of Compound	Parent/analogue
14	TC00000014	Parent
06	TC00000006	Parent
04	TC00000004	Analogue of 06
02	TC00000002	Parent
10	TC00000010	Parent
08	TC00000008	Analogue of 10
12	TC00000012	Analogue of a compound tested but not sent by ELF

Notes: The ADM-receptor antagonist compounds and their associated names/numbers

## 2.4. Cell viability assays

### 2.4.1. MTT Assay

The MTT, 3-(4,5-dimethylthiazol-2-yl)-2,5-diphenyltetrazolium bromide, assay is used to measure cell viability and can therefore indicate the cytotoxicity of a compound. MTT is a yellow tetrazolium dye and is reduced to formazan in the cell by mitochondrial reductases, as well as other cellular enzymes (Bernas & Dobrucki, 2002). Formazan forms a precipitate that is dissolved by the addition of a solubilisation solution, to form a purple colour. The reaction in which MTT is reduced to formazan is shown in Figure 2.1.

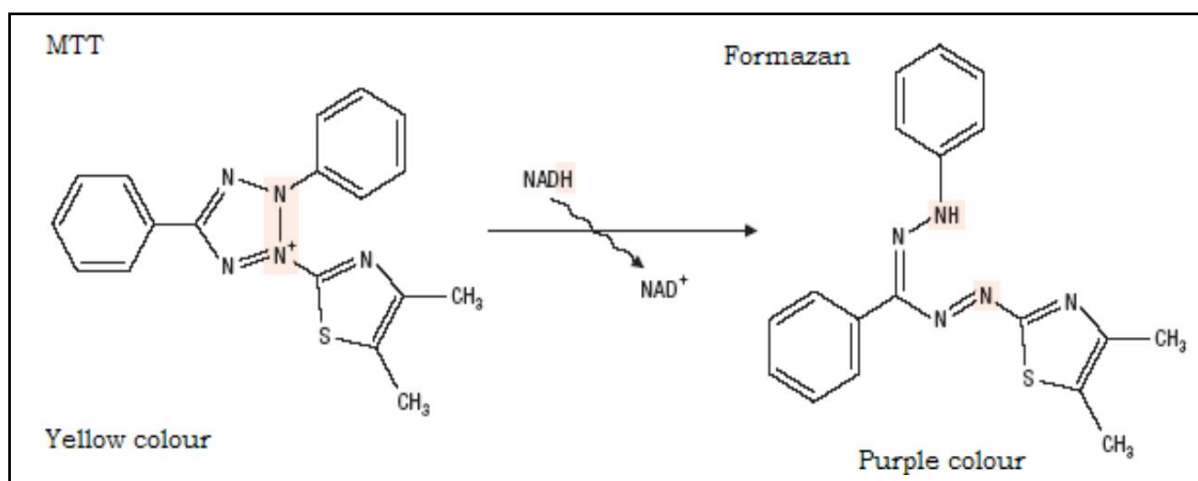


Figure 2.1. MTT reduction to form Formazan

Notes: Image was taken from figure 2 of (Desai et al., 2011)

This assay was used to investigate the effects of the compounds on cell metabolism and viability and so give an indication of the toxicity of the compounds and so their suitability as a drug. THP-1 cells were used as they are monocytes and so to some degree, although not perfectly, replicate the effect of the compounds in the blood.

The CellTiter 96 Non-Radioactive Cell Proliferation Assay kit (Promega, Wisconsin, USA) was used to perform the MTT assay. In preparation, THP-1 cells were stimulated with the cytokine, interferon- $\gamma$  (IFN- $\gamma$ ) and plated out on a 96-well plate (Sarstedt, Nümbrecht, Germany) at 100  $\mu$ L per well. Controls of stimulated THP-1 media, but no cells, were also plated out at 100  $\mu$ L per well. The cells were treated with the ADM receptor antagonist compounds at concentrations from 0.002 to 50  $\mu$ M and the plate was incubated for 24 hours at 37  $^{\circ}$ C. Fifteen  $\mu$ L dye solution was added to each well and the plate was incubated for a further 2 hours. One hundred  $\mu$ L solubilisation solution was added to each well and the plate was incubated overnight on an orbital shaker. The plate was read at 570 nm (Tecan Infinite F50 absorbance plate reader).

After the initial two hours' incubation, the purple formazan precipitate was visible in the wells containing cells. The precipitate dissolves after the addition of the solubilisation solution, giving a colour change of the solution in the well from yellow to purple. It was ensured that the precipitate was fully dissolved before the plate was read.

#### 2.4.2. CellTiter-Glo Luminescent Cell Viability Assay (Metabolism)

The kit used for cell metabolism assays was the CellTiter-Glo<sup>®</sup> Luminescent Cell Viability Assay (G7572 - Promega, Wisconsin, USA). The assay gives a measurement of the amount of intracellular ATP and therefore an indication of cellular metabolism and cell viability. The assay reagent causes cell lysis and therefore intracellular ATP to be released. ATP is required for the luminescent reaction of the luciferase enzyme, converting luciferin to oxyluciferin. As a result, the greater the luminescence signal, the greater the amount of ATP, indicating a higher percentage of viable cells. A summary of the reaction is shown in Figure 2.2.

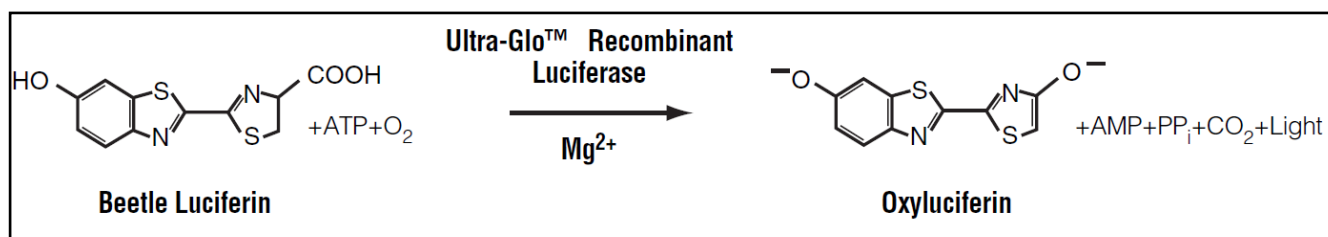


Figure 2.2. Principle reaction of the CellTiter Glo assay

Notes: Image taken from figure 3 of CellTiter-Glo® Luminescent Cell Viability Assay protocol. The luciferase enzyme oxidises luciferin to form oxyluciferin. The reaction produces light and uses ATP. Therefore the more ATP that is available, indicating more cells are viable, the more light is produced. This means the more viable cells there are, the stronger the luminescent signal.

Cells and media were plated out identically to that of the cell proliferation assay in section 2.3, in a white bottomed plate. The plate was incubated for 24 hours at 37 °C, as for the proliferation assay. One hundred µL CellTiter Glo reagent (prepared from CellTiter Glo substrate and CellTiter Glo buffer) was added to each well. The plate was gently shaken for 2 minutes and incubated at room temperature (18-25 °C) for 10 minutes. The plate was read using the GloMax® 96 Microplate Luminometer, using the pre-set protocol: CellTiter Glo.

## 2.5. ELISAs

Enzyme-linked immunosorbent assays (ELISAs) are used to quantitatively determine the presence of specific substances in cell extracts. The assays work via competition of the specific antigen in the sample with a fixed amount of an enzyme-labelled version of the antigen, for the binding sites of the primary antibody. The primary antibodies, bound to the antigen, bind to the well of the assay plate, which is coated with secondary antibody. Unbound antigen is removed via washing. Any enzyme-labelled antigen bound to the well, will produce a blue colour when substrate is added, therefore the more unlabelled antigen there was in the cell extract sample, the less intense the colour of the well will be after incubation with the substrate.

### 2.5.1. Neopterin ELISA

In preparation for this assay, after treatment with the ADM receptor antagonist compounds, for 24 hours, THP-1 cells were placed in 1.5 mL Eppendorf tubes and microcentrifuged at 500 x g for 5 minutes. The pellet was resuspended in 1 mL cold PBS and microcentrifuged for 5 minutes at 1000 x g. Cells were lysed using 40 µL RIPA buffer and incubated for 20 minutes on ice or in the refrigerator. The samples were centrifuged for 10 minutes at 10,000 x g. The supernatant was transferred to clean Eppendorf tubes. The cell extracts were then stored at -80 °C, if not used immediately.

The kit used for this assay was the Neopterin ELISA (IBL international, ref: RE59321). Twenty µL of standard, controls or diluted sample was pipetted into separate wells. Samples are diluted according to the protein concentration of each cell extract. To each well, 100 µL enzyme conjugate and 50 µL neopterin antiserum was added. The plate was covered with black adhesive foil and incubated at room temperature (18-25 °C), on an orbital shaker (at 500 rpm), for 90 minutes.

The foil was removed and the solution was discarded from the wells. The plate was washed four times with diluted wash buffer (1:20 dilution). After each wash, the excess solution was removed by dabbing the inverted plate on paper towel.

Using a multichannel pipette, 150  $\mu$ L TMB substrate solution was added to each well. TMB is 3,3',5,5'-tetramethylbenzidine, a chromogenic compound used as a substrate for horseradish peroxidase in ELISA assays, forming 3,3',5,5'-tetramethylbenzidine diimine which has a blue-green colour (Goka & Farthing, 1987). The plate was incubated at room temperature for 10 minutes. The substrate reaction was stopped by the addition of 150  $\mu$ L of TMB Stop solution and the plate was gently shaken to mix the contents of the wells. Addition of the stop reagent resulted in a colour change of blue-green to yellow, indicating the reaction has stopped.

The optical density of each well was measured using a photometer at a wavelength of 450 nm, within 15 minutes of the addition of the stop solution.

## **2.5.2. Cyclic AMP ELISA**

### **2.5.2.1. Cell sample preparation**

THP-1 cells were pre-treated with either 0.1  $\mu$ M ADM<sub>22-52</sub> (an ADM receptor antagonist) or 10  $\mu$ M ELF antagonist compound, and incubated at 37 °C for 15 minutes. The cells were then treated with 0.1  $\mu$ M ADM peptide and incubated for a further 15 minutes at 37 °C.

For THP-1 samples, the cells were centrifuged at 500 x g for 5 minutes and the medium was removed leaving the cell pellet. The pellet was washed with PBS and centrifuged for 5 minutes at 1000 xg. The pellet was then resuspended in 120  $\mu$ L 0.1 M hydrochloric acid (HCl) with 1.0 % Triton X-100. The cells were incubated for 10 minutes at room temperature. The lysed cells were centrifuged at 10,000 x g for 10 minutes and the supernatant was collected.

For adherent cell lines, media was aspirated and the cells were washed with PBS. 250  $\mu$ L HCl-Triton X-100 was added to the cells and they were incubated for 10 minutes at room temperature. The lysed cells were centrifuged at 10,000 x g for 10 minutes, as for THP-1 samples, and the supernatant was collected.

A Bradford assay was performed, using the BioRad protein assay reagent, to determine the protein concentration of the samples. The samples were diluted with 0.1 M HCl so that the protein concentration of each sample was the same and  $\geq$  1000  $\mu$ g/mL.

### **2.5.2.2. Cyclic AMP Direct Immunoassay**

The kit used for this assay was the cAMP direct immunoassay kit (Abcam, Cambridge, UK, ab65355).

Fifty  $\mu$ L Neutralizing Buffer was added to 100  $\mu$ L each sample. To this, 5  $\mu$ L Acetylating Reagent Mix (prepared by mixing Acetylating Reagent A with Acetylating Reagent B at a ratio of 1:2) was added to each sample and vortexed immediately. The samples were then incubated for 10 minutes at room temperature, in order to acetylate the cAMP. Acetylation is important for the recognition of cAMP

by the antibody. The acetylating reagents for this reaction are usually acetic anhydride and triethylamine. To each sample, 845  $\mu\text{L}$  1 x Assay Buffer was added to dilute the acetylation reagents, giving a final volume of 1 mL and such that each sample was diluted by a factor of 10.

Samples were added to the Protein G coated plate at 50  $\mu\text{L}$  per well. 10  $\mu\text{L}$  reconstituted cAMP antibody was added to each well and the plate was incubated for 1 hour at room temperature, on an orbital shaker (set at low speed). Ten  $\mu\text{L}$  cAMP-HRP (horse radish peroxidase) was added to each well and mixed using a pipette and the plate was incubated for a further hour under the same conditions as the previous incubation. The wells were washed 5 times, using 200  $\mu\text{L}$  per well of 1 x Assay Buffer for each wash. One hundred  $\mu\text{L}$  HRP Developer was added and the samples were developed for an hour at room temperature, on an orbital shaker. The samples turned light blue at this point. The reaction was stopped using 100  $\mu\text{L}$  1 M HCl per well, which resulted in a colour change from blue to yellow. The plate was read at an OD of 450 nm.

## 2.6. cAMP-Glo™ Max Assay

The cAMP-Glo Max assay by Promega was used as an alternative assay used to measure cAMP and detect changes in cAMP concentration between untreated and treated samples. The assay uses the Ultra-Glo Recombinant Luciferase technology of the Cell Titer Glo cell viability assay. The basis for the assay is that cAMP activates protein kinase A (PKA), which uses ATP to phosphorylate its substrate. The more active the PKA, the less available ATP for the luciferase reaction where luciferin is oxidised to oxyluciferin, a reaction that results in luminescence. As a result, a higher concentration of cAMP in a sample leads to a lower luminescence value, and vice versa. The principle reactions of the assay are summarised in Figure 2.3. As this assay is dependent on ATP levels, it is worth bearing in mind that varying ATP concentrations across samples would also have an effect on apparent cAMP concentration.

Cells were counted using a haemocytometer, after first being trypsinised to form single cells in suspension and stained using Trypan-blue (Sigma-Aldrich, Missouri, USA). To perform the assay, cells were plated out at a seeding density of  $10^5$  cells per well of a 96 well white plate and incubated at 37°C for 24 hours. The media was then aspirated and the cells were washed with 100  $\mu\text{L}$  PBS. The cells were treated with 100  $\mu\text{M}$  antagonist compound for 30 minutes at 37°C. The 13-52 peptide fragment ADM agonist was added to the cells at a concentration of 1  $\mu\text{M}$  for 30 minutes at 37°C. Both the antagonists and the ADM agonist were added to the cells after dilution in complete induction buffer consisting of PBS, 50 mM  $\text{MgCl}_2$ , 500  $\mu\text{M}$  IMBX and 100  $\mu\text{M}$  Ro 20-1724 (phosphodiesterase inhibitors).

Cyclic AMP detection solution was prepared from Protein Kinase A and cAMP Glo ONE buffer at a ratio of 1 in 1000. This was added to the cells at a ratio of 1 to 4 of the treatment solution. The plate was gently shaken for 1-2 minutes to mix and incubated at room temperature for 20 minutes. Kinase Glo reagent was added to the cells at a volume equal to that of the treatment solution plus the cAMP detection solution. The plate was shaken for 1-2 minutes and incubated for 10 minutes at room temperature. The luminescence was then read using a luminometer.

Statistical analyses of the data from both the ELISA and the cAMP assay were performed using the GraphPad prism software version 7. P values were calculated to determine the significance of the results.

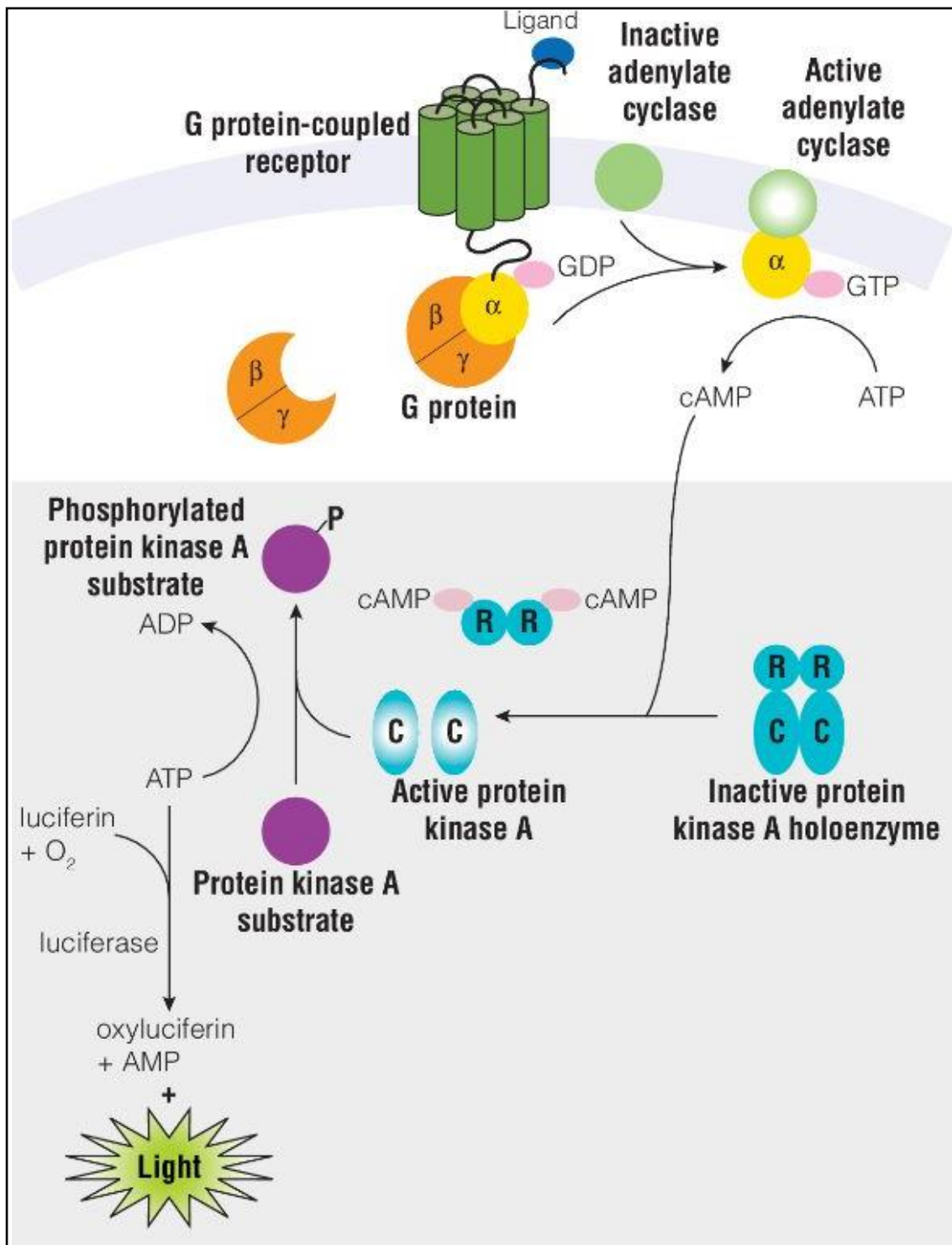


Figure 2.3. Principle reactions of the cAMP Glo Max assay

Notes: Image taken from figure 1 of the Promega cAMP Glo Max assay protocol

## 2.7. Western Blot

### 2.7.1. Sample preparation

SK N SH cells were used as they are a neuronal cell line and express the ADM receptors. Cells were plated onto 6 well plates at a seeding density of  $5 \times 10^5$  cells per well. After 48 hours, the medium was removed, the cells were washed with PBS and the medium was replaced with serum-free DMEM. The cells were pre-treated with 10  $\mu$ M ADM-receptor antagonist for 30 minutes. As a control, cells in one of the wells were pre-treated with MK2206 (an Akt inhibitor) instead of an ADM-receptor antagonist. Cells were treated with 0.1  $\mu$ M ADM<sub>13-52</sub> agonist peptide fragment and incubated for 1 hour at 37 °C. A control well of cells were also treated with a final concentration of 0.1 % DMSO, as this was equivalent to the amount of DMSO added to the antagonist treated samples. To harvest the cells, the medium was aspirated and the cells were washed with ice-cold PBS. A scraper was used to detach the cells from the surface of the plate and the cell solution was made homogenous using a micropipette. The cells were placed in a 1.5 mL Eppendorf and centrifuged at 1000 x g for 5 minutes. The supernatant was removed and the pellet was resuspended in lysis buffer, consisting of RIPA buffer, 1 % protease inhibitor cocktail and 50 mM sodium fluoride (NaF). NaF was used as a phosphatase inhibitor. The samples were incubated on ice for 20 minutes. They were then centrifuged for 10 minutes at 10,000 x g. The supernatant was removed and placed in a fresh Eppendorf. The protein concentration was determined using the Bradford assay. The protein samples were stored at -80 °C.

### 2.7.2. Western blot

Western blotting was used to analyse FoxO3 and phospho-FoxO3 (Ser253) protein content in the cell samples. 10  $\mu$ g total protein was loaded on to the gel for each sample. The low amount of protein was due to difficulties extracting a high concentration of protein from the SK N SH cells. Samples were diluted in H<sub>2</sub>O and 5  $\mu$ L loading buffer, made using 4 x Laemmli sample buffer (BioRad, Hertfordshire, UK) and  $\beta$ -mercaptoethanol (SigmaAldrich, Missouri, USA), to make a total volume of 20  $\mu$ L. They were then heated at 100 °C for 10 minutes.

SDS-PAGE gels were made to the required acrylamide percentage depending on the size of the protein of interest. For example, FoxO3 is 71 kDa therefore a gel of 10 % was used, suitable for proteins between 15 and 100 kDa. The gels were made using 40 % Acrylamide (BioRad, Hertfordshire, UK), 2 % Bis (BioRad, Hertfordshire, UK), Tris-HCl buffer, SDS, Millipore water and were set using 10 % ammonium persulfate (APS) (Sigma-Aldrich) and Temed (BioRad, Hertfordshire, UK). Samples were run on the gel for around 45 minutes at 35 mA.

Proteins were then transferred from the gel to a PVDF membrane using a semi-dry transfer apparatus (Trans-Blot® Turbo™ Transfer System, BioRad, Hertfordshire, UK). The transfer buffer contained 20 % methanol. The transfer process took 35 minutes to complete.

The membrane was then washed in Tris-buffered saline, 1 % Tween-20 (TBS-T) and blocked using SEA BLOCK blocking buffer (ThermoFisher Scientific, Massachusetts, USA) for 1 hour. This blocking buffer was chosen over traditional milk powder as milk contains caseins, a family of phosphoproteins, which would interfere with the identification of phosphor-FoxO3. The primary antibody (specific for the protein of interest) was diluted 1:1000 in the blocking buffer. The primary antibodies used for the Western blots are listed in Table 2.3. The membrane was incubated in the antibody on a plate rocker overnight on ice.

Table 2.3. Primary Antibodies used for Western blots

Antibody	Catalogue number
Phospho-FoxO3a (Ser253)	STJ90275 (St John's Laboratory Ltd., London, UK)
FoxO3a	STJ93128
GAPDH	sc-25778 (Santa Cruz Biotechnology Inc., Texas, USA)

Notes: All primary antibodies were rabbit IgG polyclonal. The secondary antibody was HRP-conjugate anti-Rabbit IgG raised in a goat host (ImmunoReagents Inc., North Carolina, USA).

The membrane was washed 6 times in TBS-T, each wash with a duration of at least 5 minutes. The secondary antibody used was HRP conjugated and diluted 1:2000 in blocking buffer. The membrane was incubated in the secondary antibody for 1 hour and a plate rocker, at room temperature. The membrane was then washed 5 times in TBS-T and once in TBS (no Tween), each wash with a duration of 5 minutes. ECL solution (BioRad, Hertfordshire, UK) was prepared by mixing solution A with solution B at a ratio of 1:1. The solution was spread evenly over the membrane before imaging.

## 2.8. Transfection of ADM receptors in SH SY5Y cells

SH SY5Y cells were seeded on a six well plate at a density of  $10^6$  cells per well. The cells were incubated for 24 hours at 37 °C. The cells were washed with PBS and the medium was aspirated and replaced with 2 mL of Opti-MEM (ThermoFisher Scientific, Massachusetts, USA). Polyethylenimine (PEI) is a chemical transfection reagent and was used to transfect the cells at a ratio of 2:1 to the DNA. A total of 2.5 µg DNA was added to each well, 1.25 µg Calcrl plasmid (Gene Bank Accession Number – AY389506) and 1.25 µg of the Ramp2 plasmid (Gene Bank Accession Number – AY265458). Plasmids were bought from the cDNA Resource Center, Pennsylvania, USA, with the cDNA for each gene having already been cloned into the pcDNA3.1(+) plasmid. PEI and DNA were diluted separately in Opti-MEM, then mixed together and incubated at room temperature for 15 minutes. The PEI:DNA mix was then added to the cells and the cells were incubated for 48 hours at 37 °C. A plasmid containing GFP cDNA was also used to transfect cells as a control.

## 3. Results

### 3.1. Gene expression in different cell lines

Gene expression was analysed in different cell lines, namely human cell lines HUVEC, SH SY5Y, SK N SH and THP-1, using quantitative real-time PCR (RT-qPCR). This was done in order to investigate the expression of adrenomedullin (*ADM*) and its associated genes; the receptor components (*CALCRL*, *RAMP2* and *RAMP3*), the binding protein (*CFH*), and *CGRPα* (*CALCA*) and its receptor (*CALCRL* and *RAMP1*). Table 3.1 shows the genes expressed in each of the cell lines tested, based on the results from the RT-qPCR. Gene expression levels were compared by assigning Cq value ranges with symbols. +++ represented a Cq value of 20-25, ++ a Cq value of 25-30, + for 30-35 and - for 35 and

over. In q-PCR, the Cq value represents the cycle number that the fluorescence - which increases as the fluorescent dye intercalates in the double stranded DNA fragments, produced from the qPCR- exceeds a set threshold. The threshold set for each qPCR was 200 RFU. A Cq value of between 20-25 was deemed to show high expression of the genes relative to each other as a Cq value of less than 20 was not achieved for any of the genes in any of the cell lines. A Cq value of over 35 was deemed to be so negligible, it was regarded that there was no expression for the particular gene of interest.

The results show that all of the cell lines express *ADM* and the *ADM*<sub>1</sub> receptor (*CALCRL* and *RAMP2*), at least at the transcriptional level, with the exception of human astrocyte cell line, 1321N1. The astrocytes analysed appeared to express the CGRP receptor (*CALCRL* and *RAMP1*) at a relatively high level in comparison to the other cell lines tested, but had little or no expression of *RAMP2* and *RAMP3*, suggesting the astrocytes do not express the *ADM* receptors. Interestingly, astrocytes showed high expression of *ADM*. All of the cell lines, with the exception of HUVEC, appear to express the *ADM*<sub>2</sub> receptor (*CALCRL* and *RAMP3*) and the CGRP receptor (*CALCRL* and *RAMP1*). Despite most of the cell lines expressing *RAMP1*, only RN46A appears to express *CALCA*, the CGRP $\alpha$  gene. The cell lines also express *AMBP-1*, also known as *CFH*. There is no data for the expression of *CFH* in the SH SY5Y cell line.

Table 3.1. Expression of *ADM* and related genes in selected human cell lines

Cell line	Gene							Key
	<i>CALCRL</i>	<i>RAMP1</i>	<i>RAMP2</i>	<i>RAMP3</i>	<i>ADM</i>	<i>CALCA</i>	<i>CFH</i>	
HUVEC	+++	-	++	-	++	-	++	Human
SH SY5Y	+	++	++	++	++	-	N/A	Human
SK N SH	+	+++	++	++	++	-	++	Human
THP-1	+	+	+	++	+	-	+	Human
Astrocyte - 1321N1	++	+++	-	+	+++	++	+++	Human

Notes: Symbols -, +, ++, +++, and N/A represent a Cq value of >35, 30-35, 25-30, 20-25, and no data respectively.

### 3.2. Cell viability and Inflammation

The MTT and CellTiter-Glo assays give an indication of cell metabolism and cell proliferation via measurement of ATP, respectively (Stockert et al., 2018; Riss et al., 2013). The assays can therefore reveal the effect of treatment with compounds, on cell viability. The results from these assays are shown in Figure 3.1. THP-1 cells were treated with 0.02  $\mu$ M, 0.2  $\mu$ M, 2  $\mu$ M, 20  $\mu$ M and 50  $\mu$ M and incubated at 37 °C for 24 hours. For all of the antagonist compounds, there appears to be no significant effect on cell viability at the three lowest concentrations (0.02  $\mu$ M, 0.2  $\mu$ M and 2  $\mu$ M) shown by the linear horizontal section of the graph at around 100 % of the maximum interassay response, at these concentrations.

For compounds TC14, TC04, TC08, TC10 and TC12, the viability of the cells had decreased after treatment with 20  $\mu$ M of compound and had further decreased after treatment with 50  $\mu$ M, to a minimum of around 50 % of that where the cells were not treated with compound. For the compounds 06 and 02, there was also a decrease in cell viability at the higher concentrations of 20  $\mu$ M and 50  $\mu$ M, however the decrease was much more rapid and the cell viability was reduced to almost 0 %, suggesting the cells were no longer viable after treatment with the higher concentrations. Bradford assays of THP-1 cell lysates after the cells were treated with the compounds TC02 and TC06, showed that the protein concentrations after cells were treated with the higher concentrations of 20  $\mu$ M and 50  $\mu$ M were much lower for these compounds compared to the other compounds at the same concentrations ( $\sim$  3 times lower).

Upon stimulation with IFN- $\gamma$ , THP-1 cells produce neopterin. Neopterin is associated with an immune response and inflammation, therefore neopterin release from THP-1 after induction by IFN- $\gamma$  is a model of inflammation. A neopterin ELISA was performed on THP-1 cells stimulated with IFN- $\gamma$  and treated with the five concentrations of the seven different compounds, incubated at 37  $^{\circ}$ C for 24 hours, in order to determine the effect of the drugs on inflammation.

For compounds TC14, TC04 and TC12, the graphs for the neopterin ELISA show that the % maximum interassay response is horizontal linear across the increasing concentration of the compounds. This suggests these compounds have no effect on inflammation or the pathway involved in neopterin production (the BH<sub>4</sub> pathway).

Compounds TC02 and TC06 appear to reduce the amount of neopterin produced, at the higher concentrations of 20  $\mu$ M and 50  $\mu$ M, to almost 0 % of that produced where no compound had been added. This suggests an ability for the compounds to reduce inflammation. However, taking into account the results from the viability assays, this reduction in neopterin is more likely to be due to cell death caused by the compounds at high concentrations. The percentage response was significantly negatively correlated to the concentration of the compound TC02 (p-value = 0.03). This suggests that the level of neopterin decreased as the concentration of compound TC02 increased.

Treatment with compounds 10 and 08 appears to result in an increase in neopterin at high concentrations, with the maximum amount of neopterin produced achieved at 50  $\mu$ M of compound. This suggests that these antagonist compounds may increase or cause inflammation via the neopterin pathway. The relative percentage of neopterin produced was significantly positively correlated to the concentration of compound TC10 (p-value = 0.04). This suggests that the level of neopterin increased as the concentration of compound TC10 increased.

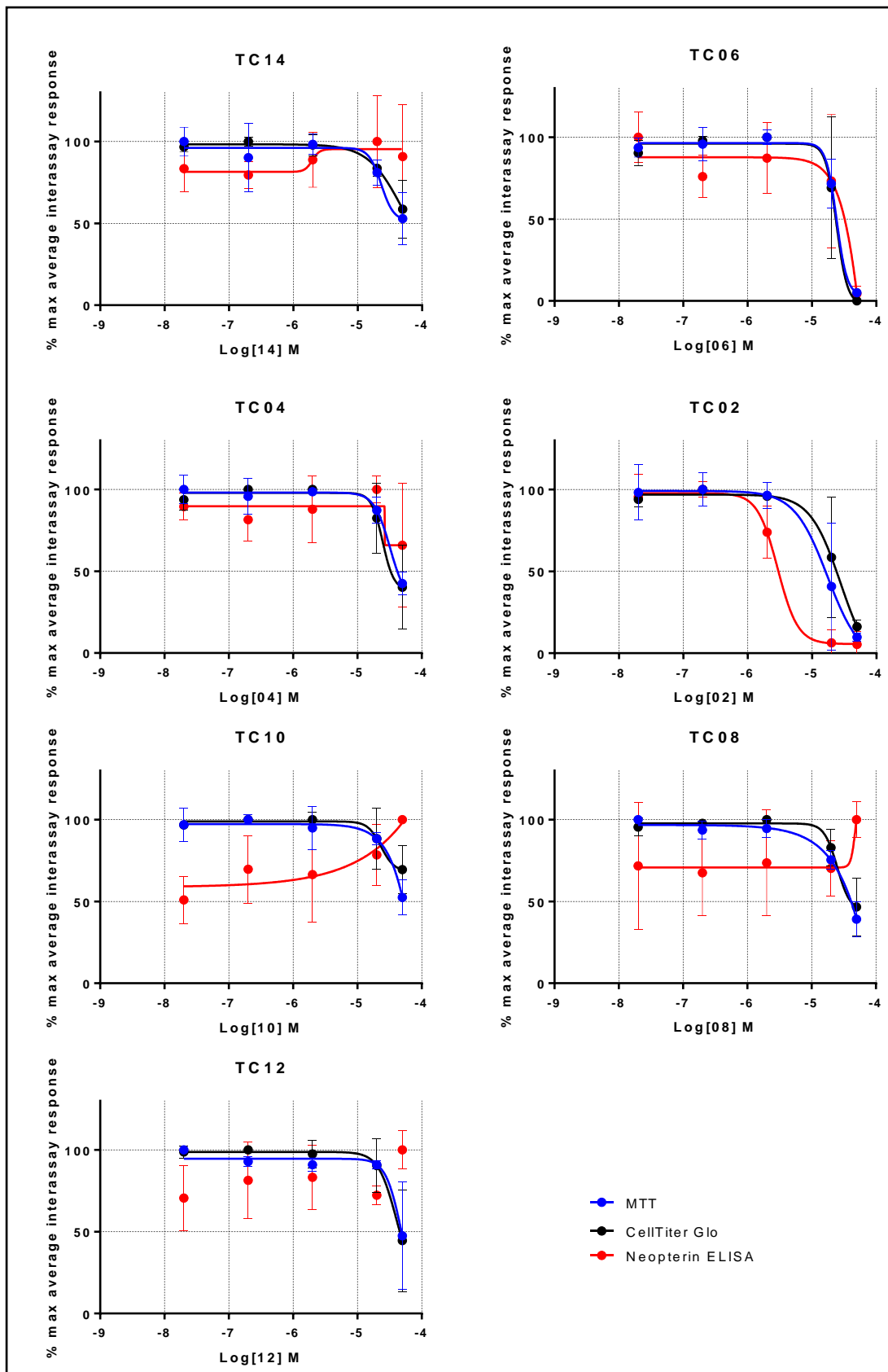


Figure 3.1. The effects of ADM receptor-antagonist compounds on cell viability and inflammation THP-1 cells were treated with 0.02  $\mu$ M, 0.2  $\mu$ M, 2  $\mu$ M, 20  $\mu$ M or 50  $\mu$ M of the antagonist compounds for 24 hours. The effects of the antagonist on cell viability were measured using the MTT and Cell Titer-Glo assays. A

neopterin ELISA was used to indicate any inflammation caused by the addition of the antagonists. For the neopterin assays, the percentage response was a measurement of the amount of neopterin, with 100 % being the maximum amount of neopterin obtained for a sample treated with a given compound. For the MTT and Cell Titer Glo assays, the percentage response was the percentage of cells viable, with 100 % being the maximum percentage of viable cells compared to the control for a given compound. Maximum interassay response refers to the relative percentage of response from the assay with 100 % being the max response from any of the assays at any given concentration of compound. This allows a comparison between the different assays.

### 3.3. Cyclic AMP levels

#### 3.3.1. cAMP ELISA

A cAMP ELISA (cAMP Assay Kit - Direct Immunoassay, Abcam, Cambridge, UK, ab65355) was used to measure the concentration of cAMP in cell samples treated with 0.1  $\mu\text{M}$  ADM and 0.1  $\mu\text{M}$  ADM with 10  $\mu\text{M}$  ADM receptor antagonist compounds or 0.1  $\mu\text{M}$  peptide antagonist, ADM<sub>22-52</sub>. The cell lines used in this initial ELISA were THP-1, SH SY5Y and the human astrocyte cell line, 1321N1. These cell lines were chosen based on the gene expression analysis results shown in Table 3.1. The gene expression analysis suggested that the cell lines expressed at least one of the ADM receptors. The aim of this ELISA was to test for the presence of a functional ADM receptor that could activate the G $\alpha$ s protein and therefore, stimulate cAMP production. The ELISA would also suggest which of the antagonist compounds could inhibit the ADM receptor most effectively.

The results of the ELISA are shown in Figure 3.2. The concentration of cAMP was very low in most of the samples, with some samples having a cAMP concentration lower than the range of the cAMP standard and therefore these results are not accurate. There was also a lot of variation between sample repeats, resulting in large error bars. The THP-1 samples had a higher average concentration of cAMP than for the SH SY5Y and astrocyte samples. The average cAMP concentration of the THP-1 samples was 7.71 fmol/ $\mu\text{L}$ , whereas the average for SH SY5Y and astrocyte samples (excluding samples stimulated with forskolin) was 0.124 fmol/ $\mu\text{L}$  and 0.572 fmol/ $\mu\text{L}$  respectively. This may be due to the possibility that the THP-1 RPMI media may contain cAMP (>350 fmol/ $\mu\text{L}$ ), according to the assay protocol (Abcam, Cambridge, UK), and some of the cAMP might have remained in the samples.

To act as a positive control, cells were treated with 5  $\mu\text{M}$  forskolin, with no ADM. Forskolin is an activator of adenylate cyclase and so should stimulate an increase in intracellular cAMP. Forskolin treatment successfully increased cAMP in SH SY5Y and astrocyte cells. The graph appears to show that cAMP levels have decreased in astrocytes treated with Forskolin however, this is due to the 'negative' values achieved for the concentration of cAMP in the untreated control, resulting in an apparently negative percentage cAMP value for the Forskolin treated cells. The average cAMP concentration for SH SY5Y cells and astrocytes stimulated with forskolin was 32.6 fmol/ $\mu\text{L}$  and 40.1 fmol/ $\mu\text{L}$  respectively. However, forskolin failed to increase intracellular cAMP levels in THP-1 cells.

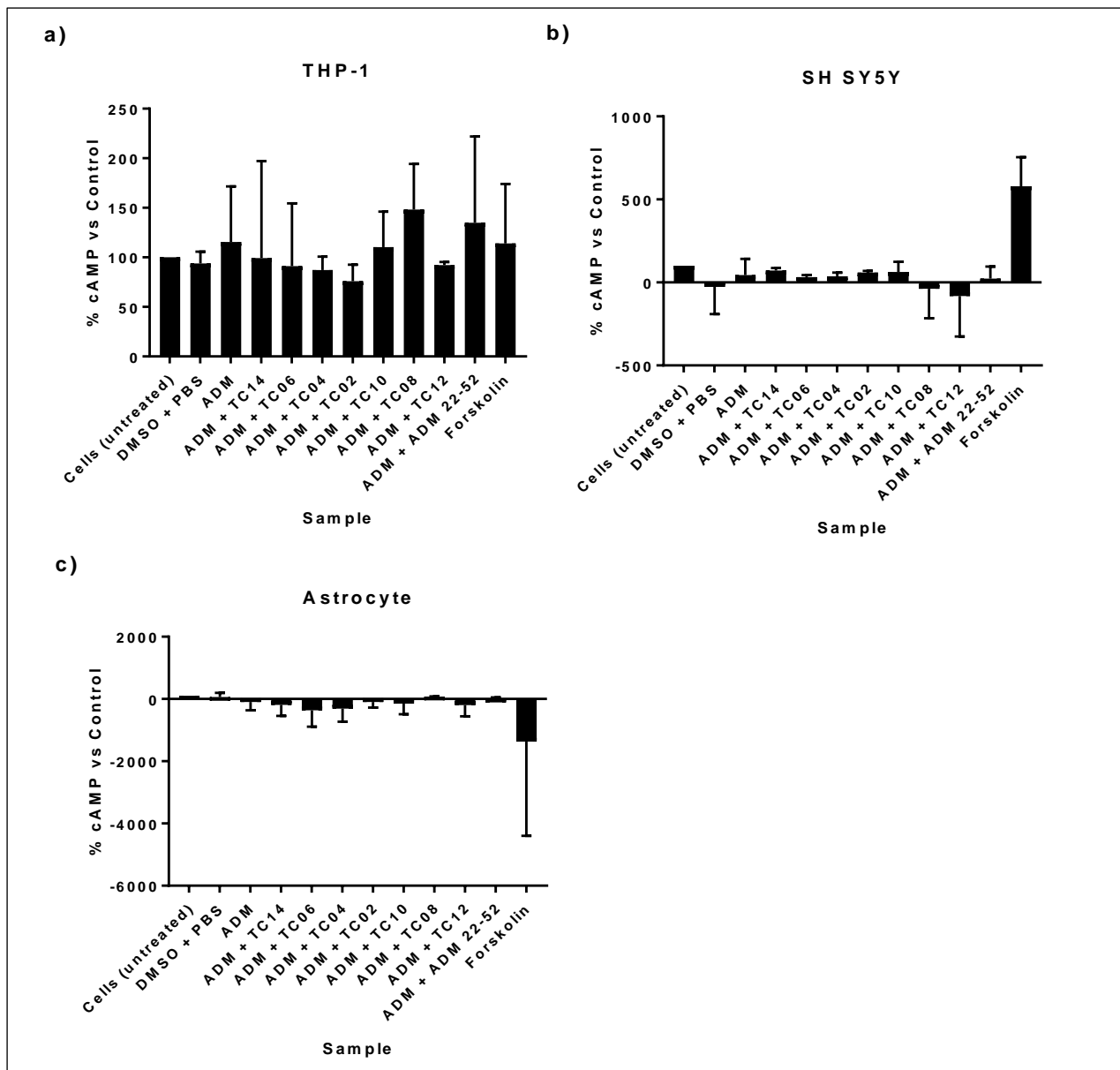


**Figure 3.2. Initial cAMP ELISAs for different cell lines treated with ADM and the receptor antagonists**  
 Results from the initial cAMP ELISA, measuring cAMP concentrations in THP-1, SH SY5Y and astrocytes treated with 0.1  $\mu$ M ADM and 10  $\mu$ M of the antagonist compound. Cells were also treated with 10  $\mu$ M forskolin as a positive control. There were three technical replicates for each sample.

### 3.3.2. cAMP-Glo Max Assay

The cAMP Glo Max assay (Promega, Wisconsin, USA, V1681) was used to measure cAMP after difficulties with the ELISA, involving presumed degradation of the IgG proteins on the assay plate meaning the kit could not be stored (contrary to the manufacturer's protocol). SK N SH cells were chosen due to their expression of the ADM receptors shown in the gene expression analysis (Table 3.1). The cells have also been shown to express the ADM receptors by Xu and Krukoff in 2005 (Xu & Krukoff, 2005). Human umbilical vein endothelial cells (HUVECs) were originally chosen as they only express the ADM<sub>1</sub> receptor and not the CGRP receptor. However sufficient cells required for the assays could not be cultured and maintained efficiently.

Results from the first biological replicate (Figure 3.3) suggest that TC14 and TC02 are the only two antagonist compounds to have greatly inhibited ADM-mediated intracellular cAMP increase. Cells treated with 1.0  $\mu$ M ADM only had an intracellular cAMP concentration of 31.3 nM, whereas cells pre-treated with 100  $\mu$ M TC14 or TC02 had intracellular cAMP concentrations of 0.7 nM and 5.3 nM respectively. TC04 appears to have the opposite effect on cAMP concentration, apparently increasing cAMP even further than ADM. The intracellular cAMP concentration of cells pre-treated with 100  $\mu$ M TC04 was 42.0 nM.

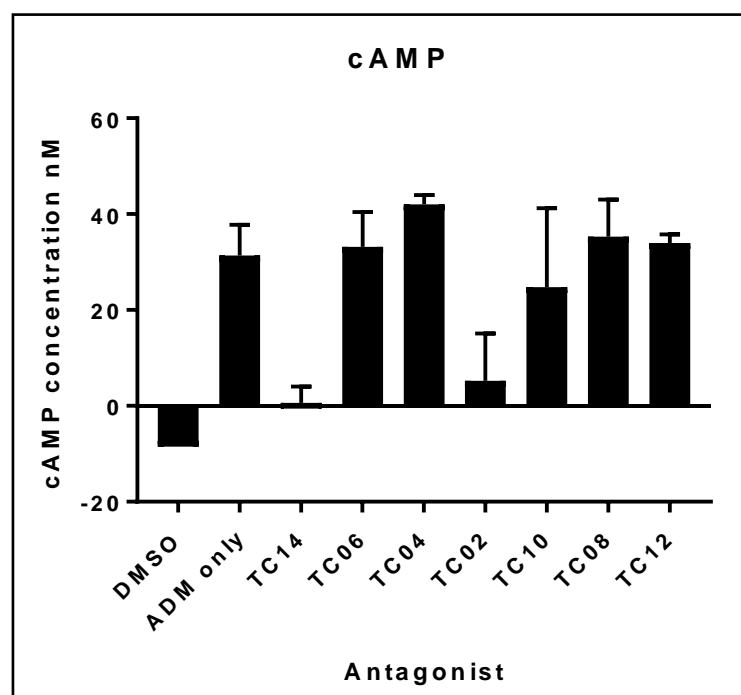


Figure 3.3. Intracellular cAMP concentration after treatment with ADM and receptor antagonists – First biological replicate

Intracellular cAMP concentrations of SK N SH cells treated with 1.0  $\mu$ M ADM for 30 minutes after pre-treatment with 100  $\mu$ M of the indicated ADM receptor antagonist compound. This was the first biological replicate with three technical replicates for each sample. To the DMSO control, 1 % DMSO was added to the cells, as this is equivalent to the total amount of DMSO in the samples treated with antagonist.

These results were not reproduced when the assay was performed again. The second biological replicate (Figure 3.4) produced results with large error bars and ADM does not appear to have stimulated cAMP production in the ADM only sample. The concentration of cAMP in the samples treated with ADM and 100  $\mu$ M antagonist appears to have increased, suggesting ADM has

stimulated cAMP synthesis in these samples. The cells treated with TC04 seem to have a higher concentration of cAMP than the other samples as was seen in the results of biological replicate one. Other than this, none of the samples have replicated the results obtained from the first replicate.

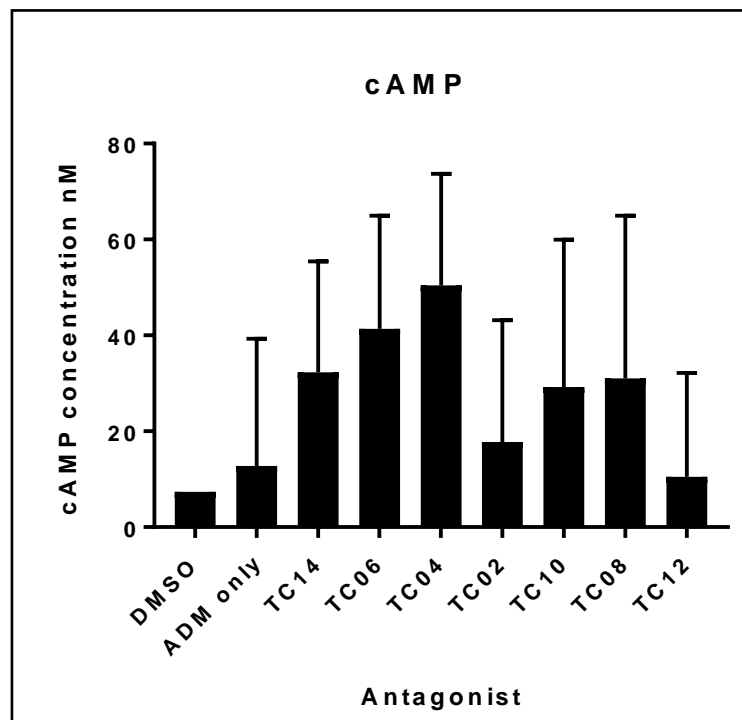


Figure 3.4. The second biological replicate of the cAMP-Glo Max assay

This was the second biological replicate with three technical replicates for each sample. The assay conditions were the same as for the first biological replicate.

### 3.4. Gene expression in SK N SH cells treated with antagonists and ADM

The expression of the ADM<sub>1</sub> receptor genes (*CALCRL* and *RAMP2*) and cyclin B1 (*CCNB1*) was investigated using RT-qPCR. SK N SH cells were treated with ADM<sub>13-52</sub> only or ADM<sub>13-52</sub> after pre-treatment with one of the antagonist compounds. Analysis of the expression of the ADM<sub>1</sub> receptor genes (graphs a and b, Figure 3.5) suggest both of the receptor genes may be down regulated in cells treated with ADM. The expression of *CALCRL* and *RAMP2* in ADM-treated cells has decreased to around 0.5 relative to their expression in non-treated cells. The pre-treatment of cells with an antagonist compounds appears to have abrogated the decrease in expression to varying degrees for each compound. The error bars are large therefore it is difficult to determine, with certainty, which compounds were most effective at preventing the decrease in expression of the receptor genes. However, it does appear that compounds TC - 02, 10, 08 and 12 (for *CALCRL*) and TC - 04, 02, 10, 08 and 12 (for *RAMP2*) were most effective at blocking the decrease in expression, bringing the expression to around that of the non-treated cells. TC14 and TC06 have resulted in a higher expression of the receptor genes than in cells treated with ADM alone, however the expression is still lower than that in the non-treated cells. In regards to *CALCRL* expression, TC04 has also failed to

bring the expression back to the level of the non-treated cells. Again, there are large error bars, particularly for TC14, which overlap the non-treated cell expression. Therefore, TC14 may have also brought the expression of the genes back to the non-treated level.

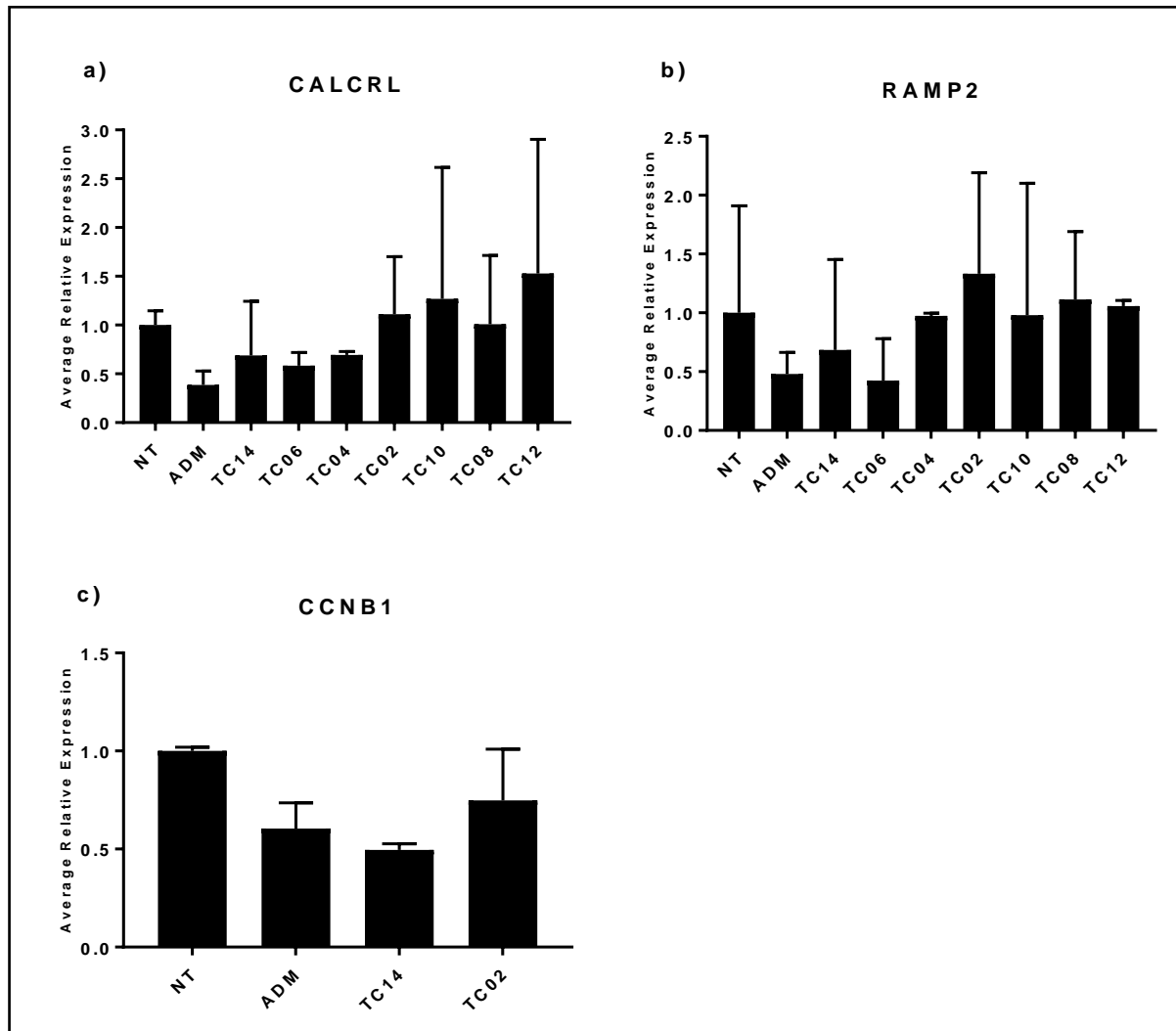


**Figure 3.5. Relative expression of ADM1 receptor genes (CALCRL and RAMP2) and Cyclin B1 (CCNB1)**  
SK N SH cells were pre-treated with 10  $\mu$ M of antagonist for 30 minutes and treated with 0.1  $\mu$ M of ADM<sub>13-52</sub> agonist peptide for 6 hours. Quantitative PCR was performed on two technical replicates for each sample, in duplicate. Gene expression was normalised to a reference gene (GAPDH) and expression in the treated samples was compared to that of the non-treated control.

The expression of cyclin B1 (*CCNB1*) (graph c, Figure 3.5) also appears to have been reduced by ADM-treatment, to around 0.6 of the expression in non-treated cells. Paradoxically, in cells pre-treated with TC14, *CCNB1* expression is even lower at 0.5. Pre-treatment with TC02 however, appears to have resulted in the expression of cyclin B1 back to around 0.75 of that of non-treated cells.

### 3.5. Western Blot

One of the project aims was to investigate potential alternative pathways involved in ADM-mediated activity, and investigate the hypothesis that the neuroprotective effect of ADM is dependent on FoxO3a phosphorylation.

On the manufacturer's website ([www.stjohnslabs.com](http://www.stjohnslabs.com) – accessed 19/07/18, STJ93128) it states that FoxO3a has a molecular mass of 97/71 kDa and shows the antibody producing a band at around 70 kDa and 85 kDa on two different Western blots using different cell lines. Based on this it is reasonable to assume that the bands indicated with arrows in Figure 3.6, between 75 and 100 kDa, correspond to FoxO3a. There are also a number of other, fainter bands at lower molecular masses and dark dots across the membrane suggesting non-specific binding. Due to the bands being unclear, it is difficult to make any obvious conclusions on the comparison of the levels of FoxO3a between the different samples. Analysis based on the intensity of the bands, using the image report function of the Image Lab software (BioRad, Hertfordshire, UK), suggested that the level of the housekeeper protein GAPDH was even across the different samples. The standard deviation of the intensity of the GAPDH bands was 0.08 where the average of the band intensities is defined as 1.

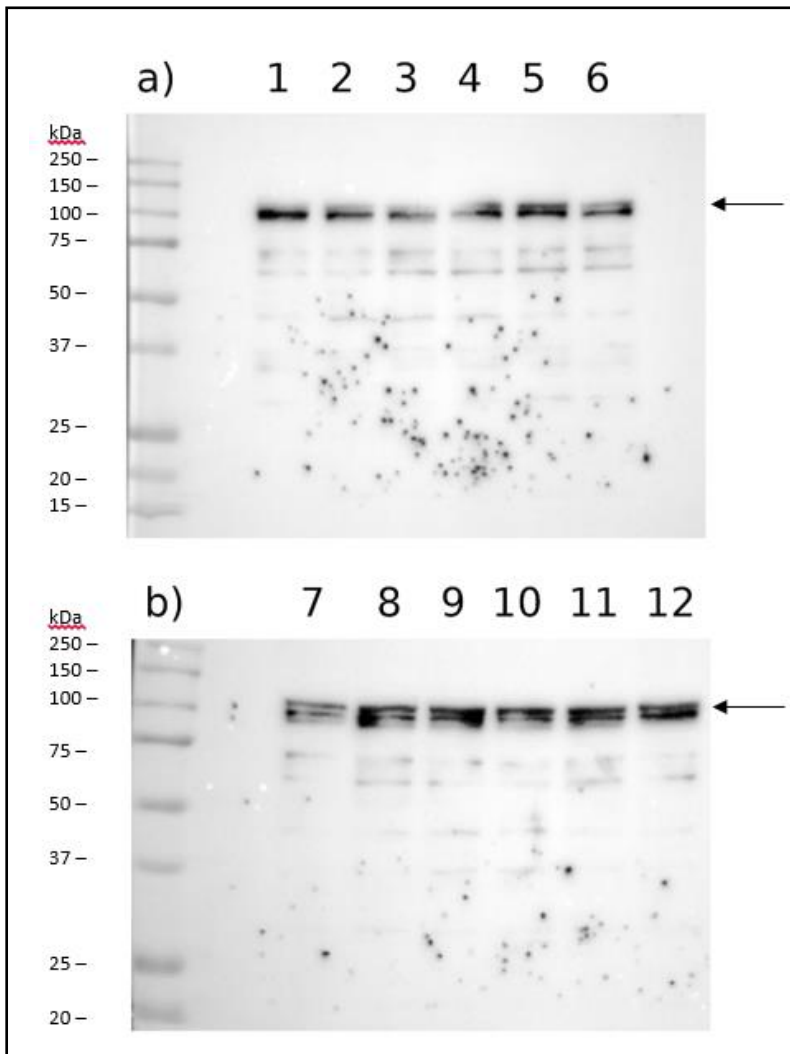


**Figure 3.6. FoxO3a\* in SK N SH cells treated with ADM and antagonist**

1 – Non-treated, 2 – DMSO (antagonist vehicle), 3 – ADM<sup>a</sup> only, 4 – TC14 + ADM, 5 – TC06 + ADM, 6 – TC04 + ADM, 7 – TC02 + ADM, 8 – TC10 + ADM, 9 – TC08 + ADM, 10 – TC12 + ADM, 11 – MK2206 (Akt inhibitor) + ADM, 12 – SC79 (Akt activator). The arrows indicate the band believed to correspond to the FoxO3a protein. \* - Not phosphorylated at the site S253; the antibody was raised around the non-phosphorylated S253 site. <sup>a</sup> – the agonist used was the ADM<sub>13-52</sub> peptide fragment

The manufacturer's website ([www.stjohnslabs.com](http://www.stjohnslabs.com) – accessed on 19/07/2018, STJ90275) shows a band between 75 and 50 kDa labelled as pFoxO3a and states that the molecular mass of the protein is 71 kDa. Therefore, the bands indicated with the arrows in Figure 3.7 are likely to correspond to p-FoxO3a. Protein from the same samples used in the blots in Figure 3.6 was used in the Western blots in Figure 3.7 where FoxO3a phosphorylated at the serine 253 site was the protein of interest. All four gels for the Western blots were run simultaneously. As with the blots in Figure 3.6, the bands on the blots in Figure 3.7 are faint and, although obviously present, they are not clearly defined. This makes it quite unclear of any differences between the samples in terms of the level of FoxO3a phosphorylation. There are also a number of different bands visible aside from the one predicted to represent P-FoxO3a. This could be a result of non-specific binding due to the antibodies being polyclonal and potentially binding to an analogue of FoxO3a.

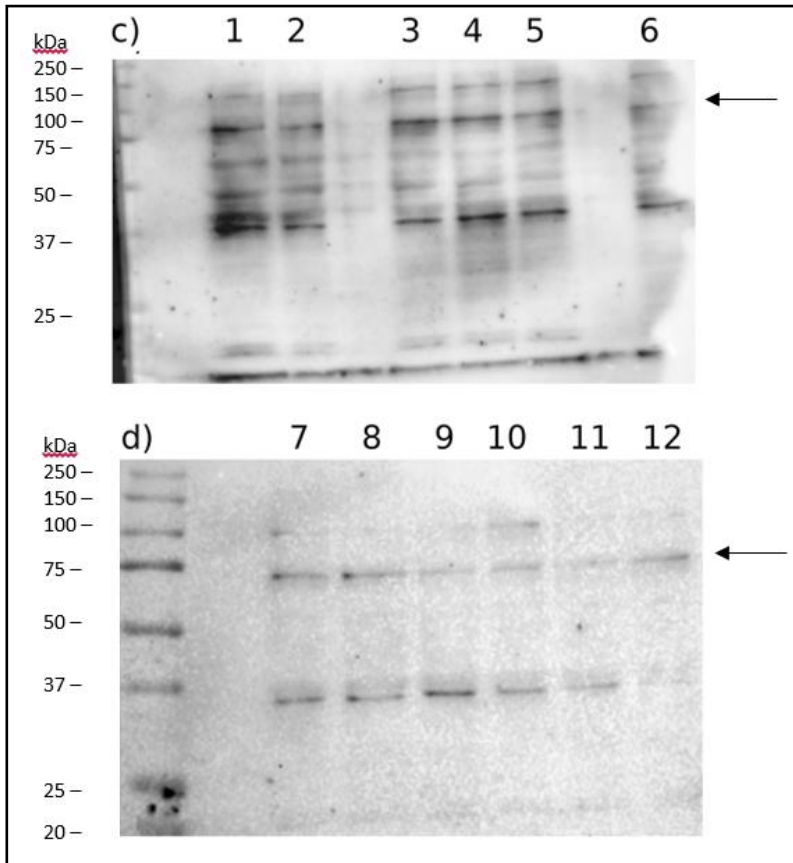


**Figure 3.7. Phosphorylated FoxO3a (S253) in SK N SH cells treated with ADM and antagonists**  
 1 – Non-treated, 2 – DMSO (antagonist vehicle), 3 – ADM<sup>a</sup> only, 4 – TC14 + ADM, 5 – TC06 + ADM, 6 – TC04 + ADM, 7 – TC02 + ADM, 8 – TC10 + ADM, 9 – TC08 + ADM, 10 – TC12 + ADM, 11 – MK2206 (Akt inhibitor) + ADM, 12 – SC79 (Akt activator). The arrows indicate the band believed to correspond to the P-FoxO3a. <sup>a</sup> –the agonist used was the ADM<sub>13-52</sub> peptide fragment

The results of densitometric analysis of the bands corresponding to either FoxO3a or P-FoxO3a compared to the bands corresponding to GAPDH, for each sample, are shown in Figure 3.8. The intensity of each band was obtained using the image report function of Image Lab software, mentioned previously. The results show the ratio of P-FoxO3a to FoxO3a in its unphosphorylated form (as the antibody used bound at the unphosphorylated Ser 253 site). The ratios for samples 7 to 12 are extremely low, with a range of just 0.03 to 0.1, suggesting a very low amount of P-FoxO3a compared to FoxO3a in these samples. The ratios for samples 1 to 6 are much larger, with a range of 0.3 to 1.3. For the non-treated control, the ratio of P-FoxO3a to FoxO3a is 0.4 and for the DMSO control the ratio is slightly higher at 0.75 suggesting that, when not treated with ADM or antagonist, more FoxO3a is in the unphosphorylated form than is in the phosphorylated form in the cell. Cells treated with ADM had a ratio of 1.3, suggesting that there is more P-Foxo3a to unphosphorylated FoxO3a and so it appears that ADM has resulted in the phosphorylation of FoxO3a. It is difficult to compare the effects of the antagonists on the ratios P-FoxO3a to unphosphorylated FoxO3a due to the low ratios for samples 7 to 12, which include the samples of cells treated with TC02, TC10, TC08 and TC12. The ratios for the cells treated with antagonists are lower than or around the same as the ratios for the controls, except for TC04, at 0.8 or below. TC14 has the highest ratio for the antagonists, at 0.8, but is still around the same as the DMSO control ratio of 0.75. However, TC04 has a higher ratio of P-FoxO3a to unphosphorylated FoxO3a than the controls, at 1.2, almost the same as the ratio for the ADM treated sample. The P-FoxO3a ratio is 0.03 in cells treated with the

Akt inhibitor, MK2206, but higher in cells treated with the Akt activator, SC79, at 0.06. No statistical analysis could be performed as the Western blot was only successfully performed once.

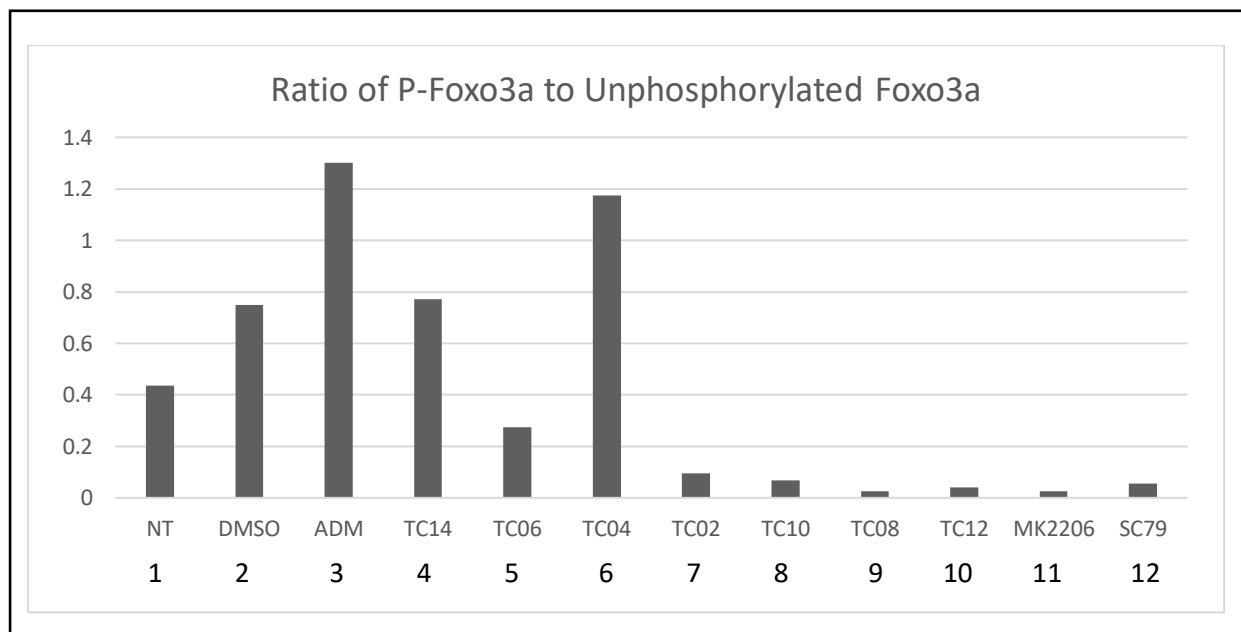


Figure 3.8. Densitometric analysis of Western Blots to show ratio of P-FoxO3a to Unphosphorylated FoxO3a

### 3.6. Transfection of ADM receptors in SH SY5Y cells

The SH SY5Y cells transfected with the GFP plasmid as a control were analysed using a microscope, under blue light. These cells were green fluorescent, indicating the transfection of these cells was successful. Protein was harvested from all of the cell samples, transfected with the different plasmids. Western blot analysis using antibodies specific for RAMP2 and CLR did not show any bands for any of the samples.

## 4. Discussion

### 4.1. Cell Viability and Inflammation

The effect of the compounds on cell viability and the induction of inflammation was assessed, before investigating their ability to inhibit ADM-mediated signalling activity. This was done using the MTT, Cell-titer Glo and Neopterin ELISA assays, and using THP-1 cells. THP-1 cells were used as they are relatively easy to maintain and grow. Furthermore, they are also of a haemopoietic lineage and so should give an indication of how the compounds would affect the body when they first enter the bloodstream. The results of the cell viability assays, MTT and Cell-Titer Glo, show that for all seven of the ADM receptor antagonist compounds there has been a reduction in cell viability at the highest

two concentrations of compound (20  $\mu\text{M}$  and 50  $\mu\text{M}$ ). This suggests that at a concentration of between 10  $\mu\text{M}$  and 20  $\mu\text{M}$  the compound begins to cause cell death. Statistical analysis showed that there was no significant correlation between the concentration of compound and cell viability (p-values  $>0.05$ ), supporting that the compounds do not cause cell death at lower concentrations. The apparent sudden induction of cell death at a concentration of between 10  $\mu\text{M}$  and 20  $\mu\text{M}$  suggests that cell mechanisms may be able to prevent damage caused by the compound, up until a threshold concentration is reached. At this point apoptosis would be triggered. A possible explanation for this could be that the compounds result in the induction of reactive oxygen species (ROS) in the cell, as cells are equipped to neutralise ROS up to a certain threshold. The purpose of the neopterin ELISA was to assess the effect of the compound on inducing inflammation, as neopterin is a pro-inflammatory marker. For compounds TC14, TC04, TC08 and TC12 the level of neopterin remains almost constant across the range of concentrations. This suggests these compounds had no effect on neopterin production and so no apparent effect on inflammation (p-values  $> 0.05$ ). For compound TC06 the level of neopterin appears to be reduced at the higher concentrations of 20  $\mu\text{M}$  and 50  $\mu\text{M}$ , suggesting the compound has reduced inflammation. However, TC06 resulted in the largest reduction in cell viability at these higher concentrations. In addition, the p-value was  $> 0.05$ , suggesting no correlation between the compound concentration and neopterin level. Therefore the observed reduction in neopterin is likely to only be a result of cell death rather than a specific reduction in the production of neopterin. Treatment with compound TC02 has also resulted in a large decrease in cell viability and an apparent large decrease in neopterin production. However, unlike for compound TC06, a reduction in neopterin is apparent at a concentration of 10  $\mu\text{M}$ . This is lower than the concentration where a reduction in cell viability is first observed, suggesting the reduction in neopterin is not just a result of cell death but rather a reduction in neopterin synthesis. This is supported by statistical analysis, showing a p-value of 0.03, suggesting there is a correlation between the concentration of TC02 and the level of neopterin. It is possible that compound TC02 affects the  $\text{BH}_4$  pathway, a pathway associated with neopterin synthesis. This finding is significant as it implies compound TC02 could reduce inflammation and affect the immune response. On the other hand, compound TC10 appears to increase neopterin levels. Statistical analysis gave a p-value of 0.04 suggesting a correlation between the concentration of the compound and neopterin levels. This suggests that compound TC10 results in increased inflammation and may elicit an immune response. This is not an ideal property for a therapeutic, particularly in the treatment of MDD which has been linked to inflammation. In particular, increased levels of pro-inflammatory markers seem to increase the probability that a patient will not respond to anti-depressant treatment (Eller et al., 2008). On the other hand, the ability of compound TC02 to reduce inflammation could therefore potentially be beneficial, if the compound could be used as a therapeutic in MDD.

## **4.2. Expression of the ADM Receptors**

Several factors have made completing the main objectives of the project more difficult than expected. One difficulty faced has been finding a cell line that both expresses the ADM receptors and does not express the CGRP receptor. After analysing cDNA from seven different cell lines (section 3.1), it appeared that HUVEC was the best candidate to fit these criteria. HUVECs only express the *Calcrl* and *Ramp2* genes, therefore only the  $\text{ADM}_1$  receptor. This was not surprising as ADM is a vasodilator and so the expression of its most specific receptor in endothelial cells would be expected. However upon culturing HUVECs, it became apparent that the cells do not grow very quickly or to a high passage number. This made it difficult to grow enough cells for the desired

assays. Endothelial cell growth medium is also relatively expensive compared to other growth media; therefore growing the cells on the scale required would not have been sustainable. In addition, endothelial cells are not the most appropriate cell line in the context of this project, as they are not particularly relevant to MDD.

Based on the gene expression analysis (Table 3.1), SH SY5Y and THP-1 cell lines appeared to express the ADM receptors and CGRP receptor, whereas the astrocyte cell line - 1321N1 appeared to mainly express the CGRP receptor. However, the cAMP ELISA results (section 3.3.1) showed that ADM did not stimulate an increase in intracellular cAMP levels in these cell lines. This suggests that, although *CALCRL* and the RAMP genes are being expressed, this is not translating to the formation of a functional receptor capable of being activated by an ADM peptide agonist. This may be because the translational or post-translational processes involved in the receptor formation require machinery not present in these cell lines or are being downregulated in by unknown factors.

The SK N SH cell line seemed to express *CALCRL* and all three RAMP genes in the gene expression analysis (section 3.1.). ADM stimulation had also previously been shown to increase nitrite and intracellular cAMP levels in SK N SH cells (Xu & Krukoff, 2005), suggesting the presence of ADM receptors. The cell line is dopaminergic neuronal and so is relevant in the context of MDD. For these reasons, SK N SH was chosen as the next cell line to investigate ADM-mediated activity.

### **4.3. ADM-Mediated cAMP Production and the Effects of Antagonist Pre-Treatment**

Measurement of cAMP levels using the cAMP ELISA (Abcam, Cambridge, UK) could not be repeated, due to the rapid degradation of the plate once opened. Therefore, the cAMP-Glo Max assay was used for further experiments. Similarly to HUVECs, SK N SH are quite slow growing cells and do not appear to reach a high level of confluency. However, for this assay, it was possible to grow enough cells to perform each repeat. A small-scale test involving only non-treated and 1.0  $\mu\text{M}$  ADM<sub>13-52</sub> treated SK N SH cells confirmed that ADM increased intracellular cAMP in this cell line.

ADM is an unstable peptide, with a half-life of just minutes (Hinson et al., 2000). It is thought that the peptide had degraded in storage at -80 °C, in PBS buffer. This was because the full length ADM peptide was able to stimulate cAMP level increase immediately after reconstitution in PBS buffer prior to freezing, but aliquots that had been frozen no longer had an effect on cAMP levels. This was also assumed to be true for the ADM<sub>22-52</sub> antagonist peptide. As a result, for experiments involving SK N SH cells (the cAMP-Glo Max assay and Western Blots) the ADM<sub>13-52</sub> peptide fragment was used as an agonist and the ADM<sub>22-52</sub> peptide could not be used as a known antagonist control, as was originally planned.

For the cAMP Glo Max assay, a calculating error meant that the cells were pre-treated with a concentration of 100  $\mu\text{M}$  of antagonist compound, instead of the intended 10  $\mu\text{M}$ . 10  $\mu\text{M}$  was originally chosen because at this concentration no cell death was observed, for any of the compounds, in the cell viability assays. Despite the high concentration of antagonist actually added to the cells, the assay appears to have been successful for the first biological cell replicate. There is nothing to suggest that cell death may have occurred, as would be expected from the results of the viability assay. This may be due to a different cell line being used in this assay compared to the

viability assays. However, it may be due to the cells in the cAMP Glo Max assay only being exposed to 100  $\mu\text{M}$  of compound for around 1 hour in total, whereas in the viability assays the cells were exposed to the compounds for 24 hours. For the cAMP assay, the cells were pre-treated with antagonist compound to ensure the antagonists to bind to the ADM receptors before ADM agonist was added and reach dissociation equilibrium. ADM agonist was added at a concentration of 1.0  $\mu\text{M}$  to ensure the maximum response was reached, based on the literature (Hay et al., 2004). The time chosen for ADM agonist stimulation was 30 minutes as this was considered long enough to activate the ADM receptor and stimulate adenylate cyclase to produce cAMP. This decision was made based on the literature (Nikishimi et al., 1998; Shimekake et al. 1995) and seemed effective. When treated with ADM agonist and each of the different antagonist compounds (section 3.3.2), only the compounds TC02 and TC14 greatly reduced cAMP. TC14 in particular has reduced the concentration of cAMP almost to 0 nM. There is concern that the decrease in cAMP may be due to cell death as the compounds TC02 and TC06 showed significant reduced cell viability at higher concentrations of 20 and 50  $\mu\text{M}$  (section 3.2.), and the concentration of compound used in the cAMP assay was higher than this at 100  $\mu\text{M}$ . However, TC06 does not show decreased cAMP as would be expected if the reduction of cAMP was due to cell death rather than inhibition of ADM activity. Cell death would also not explain the results shown for TC14, as the compound did not show a large reduction in cell viability at higher concentrations. It is worth noting that the cells used for the viability assay were of the THP-1 cell line and not SK N SH so it might be that TC14 affects SK N SH viability and not THP-1 viability and likewise TC06 affects THP-1 viability but not SK N SH viability, but this seems unlikely. Interestingly, TC04 appears to have resulted in a slight increase in cAMP compared to cells treated with ADM alone. It may be that some property of the structure of the TC04 compound is affecting luminescence. It is unlikely that the compound would produce luminescence by itself. Another explanation for the increase of cAMP caused by TC04 is that the compound could bind to ADM and result in a conformation more favourable for receptor binding and/or activation. A further explanation would be that TC04 can stimulate cAMP synthesis independently of ADM either via the ADM receptor or a different mechanism. The latter could explain why the ELF report did not pick up on the ability of TC04 to increase cAMP, because their experiments used cell lines with the ADM<sub>2</sub> receptor stably transfected into the cells and TC04 maybe be acting on a pathway not present in these cells but present in SK N SH cells. To investigate this the concentration of cAMP should be measured in cells treated with TC04 in the absence of ADM.

The results of the cAMP-Glo Max assay could not be statistically analysed to prove their significance as there were only two biological replicates performed. However, the results from the first biological replicate (Figure 3.3) showed quite clearly that the compounds TC14 and TC02 inhibited the stimulation of cAMP synthesis by the ADM agonist peptide. The error bars for the results of the first biological replicate are small, certainly much smaller than the error bars for the results for the second biological replicate (Figure 3.4). This suggests the results for the first replicate are more precise and more reliable, and so probably more accurate than the second replicate. However this is not a certainty as the assay may have intrinsic background noise and thus correct data could have large error bars in this instance. Despite this, I believe the first replicate is more likely to be correct based on many previous experiments in the literature, referenced throughout this thesis, strongly supporting that ADM is able to increase cAMP levels in cells. The assay was performed for a third time but the results were even more variable than for the second replicate. Based on this, it may be that the kit is most reliable immediately after the initial preparation of the reagents, despite storing unused reagents as specified by the protocol.

A possible explanation for only TC14 and TC02 showing significant inhibition of the ADM-mediated increase in the intracellular cAMP concentration is that the ADM peptide was in fact stimulating the

CGRP receptor. Due to cross specificity across the receptors, ADM can also act as an agonist for the CGRP receptor. Gene expression analysis (Table 3.1) showed that SK N SH express all three RAMP genes and *RAMP1* (the RAMP component that forms the CGRP receptor along with CLR) appears to be expressed at the highest level. It could be that the cAMP increase observed upon ADM treatment is a result of the collective stimulation of all three of the receptors. However ELF only tested the antagonist compounds against the ADM<sub>2</sub> receptor and so the specificity of the compounds for the CGRP receptor and the ADM<sub>1</sub> receptor is unknown. It may be that TC14 and TC02 are more specific for the CGRP receptor and, as this is the receptor that appears to be most highly expressed in SK N SH, the inhibition of increased cAMP was most apparent in cells treated with these antagonist compounds.

#### 4.4. Gene Expression of Cells Treated with the Antagonists

The results of the gene expression analysis of SK N SH cells treated with the antagonists and ADM<sub>13-52</sub> (graphs a and b, Figure 3.5) suggest that treatment with ADM agonist alone may result in decreased expression of the ADM<sub>1</sub> receptor genes (*RAMP2* and *CALCRL*). There are large error bars for some of the samples; this may be because, due to time constraints, only one biological replicate was analysed. Analysis of further biological replicates should reduce overall variability between the samples and allow statistical analysis, increasing the reliability of the results. ADM decreasing the ADM<sub>1</sub> receptor at the transcriptional level suggests an auto negative feedback mechanism for the peptide. This would provide regulation during ADM signalling pathways. The ability of the compounds to abrogate the decrease in receptor expression suggests that the compounds successfully blocked ADM signalling.

The expression of cyclin B1 (*CCNB1*) in SK N SH cells treated with ADM<sub>13-52</sub> alone or pre-treated with either TC02 or TC14 was analysed, as *CCNB1* is a gene thought to be down regulated by FoxO3a. It would be expected that, if ADM inhibits FoxO3a transcriptional activity, cells treated with ADM would have increased *CCNB1* expression. However, the results of the expression analysis for *CCNB1* (graph c, Figure 3.5) suggest that *CCNB1* expression has decreased in cells treated with ADM agonist. Furthermore, pre-treatment with the antagonist TC02 resulted in some rescue of *CCNB1* expression supporting that ADM signalling resulted in the decreased expression. However, this cannot be certain as cells pre-treated with TC14 had an even lower level of *CCNB1* expression than non-treated cells. Analysis of more biological replicates are needed to confirm the results. The compounds TC14 and TC02 were chosen as they were the antagonist compounds with the greatest effect on ADM-mediated intracellular cAMP levels (Figure 3.3). Interestingly, TC02 was successful in blocking the ADM-mediated changes in expression of all three of the genes investigated, supporting the compound's ability to antagonize ADM-signalling. However, TC14, which was the antagonist compound most effective at inhibiting ADM-mediated cAMP increase, was one of the least effective compounds at blocking the decrease in ADM<sub>1</sub> receptor expression and completely failed to block the decrease in *CCNB1* expression. However, the concentration of antagonist during the cAMP-Glo Max assay was 100  $\mu$ M whereas the concentration during pre-treatment for RNA extraction was only 10  $\mu$ M and so this may explain the difference in effectiveness for TC14.

If ADM signalling does result in decreased cyclin B1 expression, this would give evidence to reject the hypothesis that ADM mediates FoxO3a phosphorylation and inhibits FoxO3a transcriptional activity. It may even mean that ADM in fact increases FoxO3a transcriptional activity. On the other hand, other factors are likely to be involved in cyclin B1 expression independent of FoxO3a and may have counteracted any effect the inhibition of FoxO3a would have on the expression of this gene. The

original analysis of FoxO3a transcriptional regulation was done in DLD1 colon carcinoma cells (Eijkelenboom et al., 2013) and so FoxO3a may affect genes differently in different cell types. Also, ADM treatment, before RNA extraction, was 6 hours in duration and therefore phosphorylation of FoxO3a by ADM-mediated signalling may have ceased by this point. FoxO3a activity may even have temporarily increased to compensate for the inhibition, resulting in the observed decrease in *CCNB1* expression. To investigate this further, the effect of ADM on the other FoxO3a regulated genes could also be analysed. The effect of ADM stimulation on *CCNG2* could be investigated as this was a gene found to be upregulated by FoxO3a (Eijkelenboom et al., 2013). If the expression of this gene is upregulated by ADM, as the results suggested *CCNB1* was downregulated by ADM, this could further challenge our hypothesis of the effect of ADM on FoxO3a activity. A more effective way to look at the direct effect of ADM treatment on FoxO3a phosphorylation would be by Western blot analysis.

#### **4.5. ADM-Mediated FoxO3a Phosphorylation**

It was only possible to perform Western blot analysis for FoxO3a and P-FoxO3a, successfully, once. The densitometric analysis of these blots shown in Figure 3.8, seems to suggest that ADM successfully stimulated the phosphorylation of FoxO3a. This is shown by the ADM-only treated cells having a ratio of P-FoxO3a to unphosphorylated FoxO3a clearly higher than that for non-treated cells and cells treated with DMSO only. The ratio is also higher than 1.0 in ADM-only treated cells, suggesting these cells have more FoxO3a in its phosphorylated form than in its unphosphorylated form. This supports the hypothesis that ADM mediates the Akt-dependent phosphorylation of FoxO3a. Interestingly, TC04 pre-treated cells had a P-FoxO3a ratio that was also above 1.0, whereas cells pre-treated with the other antagonists had ratios around the same or below the ratio values of the controls. This seems to support the results shown in the cAMP assay where TC04 appears to have increased, or at least has not inhibited, ADM-mediated activity. Cells treated with MK2206, an Akt inhibitor, and SC79, an Akt activator, were designed to act as controls. For the MK2206 sample, cells were pre-treated with MK2206 and then treated with ADM. If the expected ADM-mediated increase in P-FoxO3a was blocked by MK2206 pre-treatment, this would support that the increase in P-FoxO3a was Akt-dependent. Cells treated with SC79 were expected to have a significant increase in P-FoxO3a, independent of ADM. The densitometric analysis for SC79 and MK2206 samples does show that the SC79 sample has a P-FoxO3a ratio of double that of the MK2206 P-FoxO3a ratio, suggesting the expected results for these samples have been obtained. However, it is not possible to make any definite conclusions due to the extremely low ratios obtained for samples 7-12, of which MK2206 and SC79 samples were numbers 11 and 12 respectively. As the samples pre-treated with the antagonists TC02, TC10, TC08 and TC12 were numbers 7-10, it has not been possible to definitively compare the effects of the antagonists on ADM-mediated activity. However, it does appear that all of the antagonists, with the exception of TC04, have P-FoxO3a ratio lower than that of the ADM-only treated sample. The low ratios for samples 7-12 are likely to be a result of the faint bands obtained for these samples when probed for P-FoxO3a. Whereas the GAPDH bands for the same samples and blot were of similar intensities to those of the other blots. A reason for this may be that there was a technical issue involving the measurement of the band intensities during exposure that did not occur for the other blots, rather than there being a low amount of P-FoxO3a protein. However, it is difficult at this stage to come to any conclusive statement. To confirm the results obtained for all of the samples, it will be necessary to perform more Western blots investigating P-FoxO3a and FoxO3a. Potentially using a FoxO3a antibody that binds to the protein away from a phosphorylation site to measure total FoxO3a protein, rather than unphosphorylated FoxO3a. Statistical analysis could also then be performed to support the results. More positively, the

Western blot has shown that SKNSH cells basally express FoxO3a. Even more so, the results show that the cells also express phosphorylated FoxO3a, which appears to be affected by the Akt pathway, shown by the less intense band after treatment with the Akt inhibitor MK2206 (lane 11, figure 3.7.). This supports that SKNSH cells are an ideal cell line to prove or disprove that ADM-mediate Foxo3a phosphorylation.

The Western blot, a in Figure 3.6, has two quite distinct bands at the molecular mass corresponding to the protein of interest, FoxO3a. This makes it difficult to assign the correct FoxO3a band. It may be that the different bands are FoxO3a at different stages of phosphorylation, despite the immunogen being raised against the non-phosphorylated S253. Phosphorylated proteins may be shifted in SDS-PAGE compared to their unphosphorylated counterpart, due to the phosphorylated protein having a higher molecular weight. This may have occurred as the antibody is polyclonal and so the antibodies will bind to slightly different sites on the protein meaning some may also be able to bind the phosphorylated site. Also FoxO3a is phosphorylated at other sites including T32, therefore the antibody may bind to FoxO3a where S253 is not phosphorylated but other sites may be phosphorylated. Ponceau S staining could be used to stain the PVDF membrane in future Western blots to ensure protein transfer has been even. Protein bands are stained red on the membrane after Ponceau staining, making it apparent whether protein transfer has been successful and even.

The black dots visible on the Western blots, particularly a and b of Figure 3.6, may be a result of the antibody binding to protein aggregates forming on the blot from the process of rocking the blot in the primary antibodies overnight. Although the blot was placed on ice for this stage, the ice gradually melted overnight, possibly causing the blot to become unlevelled, and so the coverage of the antibody over the blot may have been uneven. The temperature of the blot likely also increased. Together this may have promoted protein aggregation. A cold room would be ideal; however, rocking the blot in the primary antibody for only one hour at room temperature may also improve the quality of the blot.

Extracting enough protein to perform a Western blot from SK N SH cells was difficult. The ideal total amount of protein to load for a Western blot is 20-30 µg per well (according to Abcam's Western blot FAQ – [www.abcam.com](http://www.abcam.com), accessed 28/07/18). Therefore, the 10 µg loaded for the Westerns in section 3.5 was expected to be a little low. Despite this, there are bands, clearly visible (Figures 3.6 and 3.7), although the bands are too faint to make a conclusive comparison between them. Loading a higher amount of protein would potentially make the bands more visible, making them easier to analyse and so reach a conclusion on whether there are differences in FoxO3a phosphorylation between the different samples. Based on the hypothesis that ADM stimulates FoxO3a phosphorylation via the PI3K/Akt pathway, it would be expected that samples treated with ADM agonist peptide would have an increased ratio of P-FoxO3a to non-phosphorylated FoxO3a. As a positive control, cells treated with the Akt activator, SC79, should also have increased P-FoxO3a. The Akt inhibitor, MK2206, should block FoxO3a phosphorylation. The ability of the ADM receptor antagonists to inhibit ADM-mediated FoxO3a phosphorylation would give an indication of the compounds' ability to block ADM-receptor activation. Due to the slow growing nature and sensitive adherence of SK N SH cells, extracting a higher concentration of protein was not possible by growing the cells for treatment in 6 well plates, even when using plates with the Sarstedt Cell+ growth surface for sensitively adhering cell lines. Further attempts produced an even lower concentration of protein, preventing repeats of the Western blot. Using T25 flasks to culture the cells for treatment also did not produce enough protein. However, these T25 flasks did not have the Cell+ growth surface, which may explain why the protein yield was not improved compared to the yield when using 6 well plates which did have the Cell+ growth surface. The sensitively adhering SK N SH cells

are likely to have been lost during washing steps. Growing the cell samples in T25 or perhaps T75 flasks with the Cell+ growth surface may yield a higher concentration of protein, but this would require a lot of space and materials, especially if each sample is performed in triplicate.

An alternative would be to transfect the cDNA of the ADM receptor genes into cells which do not express a functional ADM receptor. This would be particularly advantageous because this method would allow the investigation of the effect of the antagonists on each of the two ADM receptors and also the CGRP receptor (to check for cross-specificity) separately. For example, cells could be co-transfected with *CALCRL* and one of the RAMP genes (*RAMP1*, *RAMP2* or *RAMP3*); this would lead to the expression of either the CGRP, ADM<sub>1</sub> or ADM<sub>2</sub> receptor, respectively. The cAMP and Western blot assays could then be repeated using each of the cell groups, transfected with the different receptors, and the effects of the antagonists on each receptor could be directly compared without the potential for cross-specificity.

#### **4.6. Transfection of Cells with ADM Receptor Components**

An attempt was made to co-transfect SH SY5Y cells with *CALCRL* and *RAMP2* (using the method in section 2.8), therefore with the aim that the transfected cells would express the ADM<sub>1</sub> receptor. The SH SY5Y cell line was chosen because it is also a neuronal cell line, actually derived from a subclone of SK N SH cells, and so is relevant to MDD. Despite being a subclone of SK N SH, SH SY5Y divide more rapidly than SK N SH and also adhere less sensitively. As a result, it was hoped that a higher concentration of protein could be extracted from the cells for the Western blot assays. Furthermore, although gene expression analysis (Table 3.1) showed that SH SY5Y expresses the receptor genes to some degree, cAMP ELISA results (Figure 3.2, graph b) and a brief test using the cAMP-Glo Max assay (data not shown) revealed that the cell line does not appear to express a functional ADM receptor. More specifically, the cell line does not express a receptor capable of stimulating cAMP synthesis in the presence of ADM.

Western blot analysis of the transfected cells did not appear to result in receptor expression. Protein extracts were analysed using antibodies raised against the CLR and RAMP2 proteins and no bands were visible. This suggests that the transfection was not successful however, it could also be that Western blot conditions have not yet been optimised. With more time, both the transfection and Western blot method could be optimised using SH SY5Y and yield better results. If this is not successful however, it may be that SH SY5Y do not possess the machinery required to synthesise a functional ADM receptor. If so, the transfection could be attempted in HEK 293 cells as this cell line is known to be relatively easy to transfect and the ADM receptors have previously been transfected in this cell line (Aiyar, Disa, Pullen, & Nambi, 2001).

#### **4.7. Conclusion**

In summary, the obstacles addressed in the discussion have made attempting to fulfil the main aims of this project more arduous than expected. The most appropriate and available cell line for investigating ADM receptor antagonists, in relation to MDD, was found to be SK N SH. The cell line expresses the ADM receptors both at the transcriptional level and as a functional receptor, capable of stimulating adenylate cyclase upon ADM binding. However, there is the possibility that cross specificity of ADM for the CGRP receptor was responsible for the results observed in the cAMP

assay. This could be investigated using HUVECs, in a small scale test, as the cells only express the ADM<sub>1</sub> receptor. The cAMP assay could also be replicated using CGRP as the peptide agonist instead of ADM and the results could be compared to see if the effects on cAMP levels are similar for the two peptides. This may suggest cross specificity was responsible for the results obtained. Regardless of this, SK N SH is still a promising and relevant cell line for the investigation of ADM mediated effects in regards to MDD.

In terms of the most promising antagonists, TC02 appears to be the most effective. The compound showed antagonism in both the cAMP assay and the gene expression analysis of *CCNB1*. These assays need to be repeated to back up the results with statistical analysis. The compound did lead to cell death in THP-1 cells at concentrations higher than 20 µM. However at lower concentrations, and potentially therapeutically relevant concentrations, there was no cell death observed. TC02 also appeared to show an ability to reduce the pro-inflammatory marker neopterin. Therefore, in terms of a potential therapeutic for MDD, the compound could act in two different ways, by reducing inflammation and blocking ADM-mediated activity. Of course, more analysis is needed to confirm the effectiveness of the compound. TC14 was also a promising antagonist in the cAMP assay but further experiments are needed to confirm the results were the result of ADM receptor inhibition and not CGRP receptor inhibition. The results of the assays have also potentially illuminated the possibility of TC04 having agonistic properties in regards to ADM activity and so this should be investigated, as this could also have potential therapeutic benefits, in situations where ADM has been shown to be protective.

Western blot experiments have shown that it is possible to identify phosphorylated FoxO3a using this technique. As a result, it should be possible to use Western blot to shed light on the effect of ADM on P-FoxO3a levels and therefore the effect of ADM on FoxO3a transcriptional activity. If the hypothesis is correct that ADM results in FoxO3a phosphorylation, this will be important therapeutically and could explain many of the effects seen regarding ADM in disease.

It is still unclear whether ADM is beneficial or detrimental in the case of MDD. It may be that the peptide is increased in MDD patients as a neuroprotective mechanism or that increased ADM exacerbates an imbalanced HPA axis, leading to increased stress. In reality, it may be a combination of these factors at play. The small molecular antagonist compounds investigated in this project may be able to be used in further research, to shed more light on the relationship between ADM and MDD, and lead to a more effective treatment for MDD.

## References

- Aiyar, N., Disa, J., Pullen, M., & Nambi, P. (2001). Receptor activity modifying proteins interaction with human and porcine calcitonin receptor-like receptor (CRLR) in HEK-293 cells. *Mol Cell Biochem*, 224(1-2), 123-133.
- Akpinar, A., Yaman, G. B., Demirdas, A., & Onal, S. (2013). Possible role of adrenomedullin and nitric oxide in major depression. *Prog Neuropsychopharmacol Biol Psychiatry*, 46, 120-125. doi:10.1016/j.pnpbp.2013.07.003
- Beltowski, J., & Jamroz, A. (2004). Adrenomedullin--what do we know 10 years since its discovery? *Pol J Pharmacol*, 56(1), 5-27.
- Bernas, T., & Dobrucki, J. (2002). Mitochondrial and nonmitochondrial reduction of MTT: interaction of MTT with TMRE, JC-1, and NAO mitochondrial fluorescent probes. *Cytometry*, 47(4), 236-242.
- Biedler, J. L., Helson, L., & Spengler, B. A. (1973). Morphology and growth, tumorigenicity, and cytogenetics of human neuroblastoma cells in continuous culture. *Cancer Res*, 33(11), 2643-2652.
- Bolander Jr, F. F. (2004). CHAPTER 7 - Membrane Receptors *Molecular Endocrinology (Third Edition)* (pp. 147-213). San Diego: Academic Press.
- Booe, J. M., Walker, C. S., Barwell, J., Kuteyi, G., Simms, J., Jamaluddin, M. A., . . . Pioszak, A. A. (2015). Structural Basis for Receptor Activity-Modifying Protein-Dependent Selective Peptide Recognition by a G Protein-Coupled Receptor. *Mol Cell*, 58(6), 1040-1052. doi:10.1016/j.molcel.2015.04.018
- Booe, J. M., Warner, M. L., Roehrkasse, A. M., Hay, D. L., & Pioszak, A. A. (2018). Probing the mechanism of receptor activity-modifying protein modulation of GPCR ligand selectivity through rational design of potent adrenomedullin and calcitonin gene-related peptide antagonists. *Mol Pharmacol*, 93(4), 355-367. doi:10.1124/mol.117.110916
- Bradley, A. J., & Dinan, T. G. (2010). A systematic review of hypothalamic-pituitary-adrenal axis function in schizophrenia: implications for mortality. *J Psychopharmacol*, 24(4 Suppl), 91-118. doi:10.1177/1359786810385491
- Corey-Lisle, P. K., Nash, R., Stang, P., & Swindle, R. (2004). Response, partial response, and nonresponse in primary care treatment of depression. *Archives of Internal Medicine*, 164(11), 1197-1204. doi:10.1001/archinte.164.11.1197
- de Graaf, C., Song, G., Cao, C., Zhao, Q., Wang, M.-W., Wu, B., & Stevens, R. C. (2017). Extending the Structural View of Class B GPCRs. *Trends in Biochemical Sciences*, 42(12), 946-960. doi:10.1016/j.tibs.2017.10.003
- DeFea, K. (2008).  $\beta$ -arrestins and heterotrimeric G-proteins: collaborators and competitors in signal transduction. *Br J Pharmacol*, 153(S1), S298-S309. doi:10.1038/sj.bjp.0707508
- Delgado, P. L. (2000). Depression: the case for a monoamine deficiency. *J Clin Psychiatry*, 61 Suppl 6, 7-11.
- Desai, S., S. Sukhramani, P., S. Sukhramani, P., R. Tirthani, S., A. Desai, S., & P. Suthar, M. (2011). Biological cytotoxicity evaluation of spiro[azetidino-2, 3'-indole]-2', 4(1'H)-dione derivatives for anti-lung and anti-breast cancer activity. *Der Pharmacia Lettre*, 2011: 3 (5) 236-243.
- Dickenson, J., Freeman, F., Mills, C. L., Sivasubramaniam, S., & Thode, C. (2013). Signalling Complexes: Protein-protein Interactions and Lipid Rafts. In *Molecular pharmacology: from DNA to drug discovery*. (pp. 339-364) Chichester: Wiley-Blackwell.
- Dickerson, I. (2013). Role of CGRP-receptor component protein (RCP) in CLR/RAMP function. *Curr Protein Pept Sci*. 2013 Aug;14(5):407-15

- Dipette, D. J., & Supowit, S. (2008). Calcitonin Gene-Related Peptides and Adrenomedullin-Derived Peptides. In J. L. Izzo, D. A. Sica, & H. R. Black (Eds.), *Hypertension Primer*: Lippincott Williams & Wilkins.
- Eijkelenboom, A., Mokry, M., de Wit, E., Smits, L. M., Polderman, P. E., van Triest, M. H., . . . Burgering, B. M. T. (2013). Genome-wide analysis of FOXO3 mediated transcription regulation through RNA polymerase II profiling. *Molecular Systems Biology*, *9*(1), 638. doi:10.1038/msb.2012.74
- Eller, T., Vasar, V., Shlik, J., & Maron, E. (2008). Pro-inflammatory cytokines and treatment response to escitalopram in major depressive disorder. *Progress in Neuro-Psychopharmacology and Biological Psychiatry*, *32*(2), 445-450. doi:<https://doi.org/10.1016/j.pnpbp.2007.09.015>
- Evans, B. N., Rosenblatt, M. I., Mnayer, L. O., Oliver, K. R., Dickerson, I. M., & II. (2000). CGRP-RCP, a Novel Protein Required for Signal Transduction at Calcitonin Gene-related Peptide and Adrenomedullin Receptors. *Journal of Biological Chemistry*, *275*(40), 31438-31443. doi:10.1074/jbc.M005604200
- Ferguson, J. M. (2001). SSRI Antidepressant Medications: Adverse Effects and Tolerability. *Primary Care Companion to The Journal of Clinical Psychiatry*, *3*(1), 22-27.
- Ferrero H, Larrayoz IM, Gil-Bea FJ, Martínez A, Ramírez MJ. (2018) Adrenomedullin, a Novel Target for Neurodegenerative Diseases. *Mol Neurobiol*, *55*(12):8799-8814. 2018a Mar 29. doi:10.1007/s12035-018-1031-y.
- Ferrero, H., Larrayoz, I. M., Martisova, E., Solas, M., Howlett, D. R., Francis, P. T., . . . Ramirez, M. J. (2018b). Increased Levels of Brain Adrenomedullin in the Neuropathology of Alzheimer's Disease. *Mol Neurobiol*, *55*(6), 5177-5183. doi:10.1007/s12035-017-0700-6
- García-Sanmartín, J., Larráyoz, I. M., Ochoa-Callejero, L., Martínez, A. (2013). *Handbook of Biologically Active Peptides* (A. Kastin Ed.). San Diego, UNITED STATES: Elsevier Science.
- Glubb, D. M., McHugh, P. C., Deng, X., Joyce, P. R., & Kennedy, M. A. (2010). Association of a functional polymorphism in the adrenomedullin gene (ADM) with response to paroxetine. *Pharmacogenomics J*, *10*(2), 126-133. doi:10.1038/tpj.2009.33
- Goka, A. K., & Farthing, M. J. (1987). The use of 3,3',5,5'-tetramethylbenzidine as a peroxidase substrate in microplate enzyme-linked immunosorbent assay. *J Immunoassay*, *8*(1), 29-41. doi:10.1080/01971528708063053
- Goodyer, I. M. (2003). *Unipolar depression: a lifespan perspective*. Oxford: Oxford University Press.
- Hay, D. L., Conner, A. C., Howitt, S. G., Smith, D. M., & Poyner, D. R. (2004). The pharmacology of adrenomedullin receptors and their relationship to CGRP receptors. *Journal of Molecular Neuroscience*, *22*(1), 105-113. doi:10.1385/jmn:22:1-2:105
- Hay, D. L., Garelja, M. L., Poyner, D. R., & Walker, C. S. (2018). Update on the pharmacology of calcitonin/CGRP family of peptides: IUPHAR Review 25. *Br J Pharmacol*, *175*(1), 3-17. doi:10.1111/bph.14075
- Herrman, H., Maj, M., & Sartorius, N. (2009). Depressive disorders. In G. I. Papakostas (Ed.), (pp. 47-74): John Wiley & Sons, Ltd.
- Joy Patricia Hinson, Supriya Kapas, David Michael Smith. (2000). Adrenomedullin, a Multifunctional Regulatory Peptide, *Endocrine Reviews*, Volume 21, Issue 2, 1 April 2000, Pages 138–167, doi.org/10.1210/edrv.21.2.0396
- Hu, W., Shi, L., Li, M.-y., Zhou, P.-h., Qiu, B., Yin, K., . . . Zhang, L.-j. (2017). Adrenomedullin protects Leydig cells against lipopolysaccharide-induced oxidative stress and inflammatory reaction via MAPK/NF-κB signalling pathways. *Scientific Reports*, *7*, 16479. doi:10.1038/s41598-017-16008-x
- Ishimitsu, T., Kojima, M., Kangawa, K., Hino, J., Matsuoka, H., Kitamura, K., . . . Matsuo, H. (1994). Genomic Structure of Human Adrenomedullin Gene. *Biochem Biophys Res Commun*, *203*(1), 631-639. doi:<https://doi.org/10.1006/bbrc.1994.2229>
- Kenyon, C., Chang, J., Gensch, E., Rudner, A., & Tabtiang, R. (1993). A *C. elegans* mutant that lives twice as long as wild type. *Nature*, *366*(6454), 461-464. doi:10.1038/366461a0

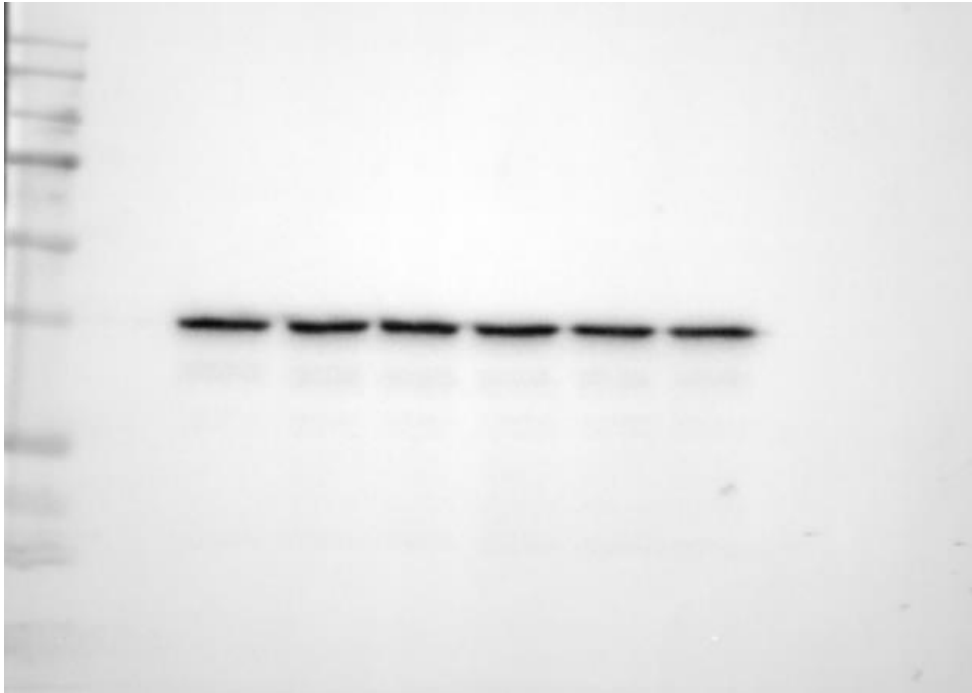
- Kiecolt-Glaser JK, Derry HM, Fagundes CP. (2015) Inflammation: depression fans the flames and feasts on the heat. *Am J Psychiatry*. 2015 Nov 1;172(11):1075-91. doi: 10.1176/appi.ajp.2015.15020152. Epub 2015 Sep 11. Review.
- Kitamura, K., Kangawa, K., Kawamoto, M., Ichiki, Y., Nakamura, S., Matsuo, H., & Eto, T. (1993). Adrenomedullin: A Novel Hypotensive Peptide Isolated from Human Pheochromocytoma. *Biochem Biophys Res Commun*, 192(2), 553-560. doi:<https://doi.org/10.1006/bbrc.1993.1451>
- Kovacs, J. J., Hara, M. R., Davenport, C. L., Kim, J., & Lefkowitz, R. J. (2009). Arrestin Development: Emerging Roles for  $\beta$ -arrestins in Developmental Signaling Pathways. *Developmental cell*, 17(4), 443-458. doi:10.1016/j.devcel.2009.09.011
- Kuwasako, K., Sekiguchi, T., Nagata, S., Jiang, D., Hayashi, H., Murakami, M., . . . Kato, J. (2016). Inhibitory effects of two G protein-coupled receptor kinases on the cell surface expression and signaling of the human adrenomedullin receptor. *Biochem Biophys Res Commun*, 470(4), 894-899. doi:10.1016/j.bbrc.2016.01.138
- Larráyoz, I. M., Martínez-Herrero, S., García-Sanmartín, J., Ochoa-Callejero, L., & Martínez, A. (2014). Adrenomedullin and tumour microenvironment. *Journal of Translational Medicine*, 12(1), 339. doi:10.1186/s12967-014-0339-2
- Lindqvist, D., Dhabhar, F. S., James, S. J., Hough, C. M., Jain, F. A., Bersani, F. S., . . . Mellon, S. H. (2017). Oxidative stress, inflammation and treatment response in major depression. *Psychoneuroendocrinology*, 76(Supplement C), 197-205. doi:<https://doi.org/10.1016/j.psyneuen.2016.11.031>
- Mahajan, G. J., Vallender, E. J., Garrett, M. R., Challagundla, L., Overholser, J. C., Jurjus, G., . . . Stockmeier, C. A. (2017). Altered neuro-inflammatory gene expression in hippocampus in major depressive disorder. *Progress in Neuro-Psychopharmacology and Biological Psychiatry*, 2;82:177-186. doi:<https://doi.org/10.1016/j.pnpbp.2017.11.017>
- Marsden, W. N. (2013). Synaptic plasticity in depression: Molecular, cellular and functional correlates. *Progress in Neuro-Psychopharmacology and Biological Psychiatry*, 43, 168-184. doi:<https://doi.org/10.1016/j.pnpbp.2012.12.012>
- Martínez, A., Julián, M., Bregonzio, C., Notari, L., Moody, T. W., & Cuttitta, F. (2004). Identification of Vasoactive Nonpeptidic Positive and Negative Modulators of Adrenomedullin Using a Neutralizing Antibody-Based Screening Strategy. *Endocrinology*, 145(8), 3858-3865. doi:10.1210/en.2003-1251
- Matteo, R. D., & May, C. N. (2003). Direct coronary vasodilator action of adrenomedullin is mediated by nitric oxide. *Br J Pharmacol*, 140(8), 1414-1420. doi:10.1038/sj.bjp.0705572
- McLatchie, L. M., Fraser, N. J., Main, M. J., Wise, A., Brown, J., Thompson, N., . . . Foord, S. M. (1998). RAMPs regulate the transport and ligand specificity of the calcitonin-receptor-like receptor. *Nature*, 393, 333. doi:10.1038/30666
- McLaughlin, C. N., & Broihier, H. T. (2018). Keeping Neurons Young and Foxy: FoxOs Promote Neuronal Plasticity. *Trends Genet*, 34(1), 65-78. doi:10.1016/j.tig.2017.10.002
- Meeran, K., O'Shea, D., Upton, P. D., Small, C. J., Ghatei, M. A., Byfield, P. H., & Bloom, S. R. (1997). Circulating adrenomedullin does not regulate systemic blood pressure but increases plasma prolactin after intravenous infusion in humans: a pharmacokinetic study. *J Clin Endocrinol Metab*, 82(1), 95-100. doi:10.1210/jcem.82.1.3656
- Merlot, S., & Firtel, R. A. (2003). Leading the way: directional sensing through phosphatidylinositol 3-kinase and other signaling pathways. *Journal of Cell Science*, 116(17), 3471-3478. doi:10.1242/jcs.00703
- Miyashita K, Itoh H, Sawada N, Fukunaga Y, Sone M, Yamahara K, Yurugi-Kobayashi T, Park K, Nakao K. (2003) Adrenomedullin provokes endothelial Akt activation and promotes vascular regeneration both in vitro and in vivo. *FEBS Lett*. 2003 Jun 5;544(1-3):86-92.
- NICE National Institute for Health and Care Excellence (2018) *Depression in adults: recognition and management Clinical Guideline [CG90]* Retrieved from

- <https://www.nice.org.uk/guidance/cg90/chapter/1-Guidance#treatment-choice-based-on-depression-subtypes-and-personal-characteristics>
- NICE National Institute for Health and Care Excellence (2019) *Anti-depressant drugs* Retrieved from <https://bnf.nice.org.uk/treatment-summary/antidepressant-drugs.html>
- Nishikimi T, Horio T, Yoshihara F, Nagaya N, Matsuo H, Kangawa K. (1998) Effect of adrenomedullin on cAMP and cGMP levels in rat cardiac myocytes and nonmyocytes. *Eur J Pharmacol*. 1998 Jul 24;353(2-3):337-44.
- Nishikimi T, Kuwahara K, Nakagawa Y, Kangawa K, Nakao K. (2013) Adrenomedullin in cardiovascular disease: a useful biomarker, its pathological roles and therapeutic application. *Curr Protein Pept Sci*. 2013 Jun;14(4):256-67. Review. PubMed PMID: 23745694
- Nor Suhaila, R., & Safuan, S. (2017). Isolation Methods and Culture Conditions of Human Umbilical Vein Endothelial Cells from Malaysian Women. *Sains Malaysiana* 46(3):463-468
- Ochoa-Callejero, L., García-Sanmartín, J., Martínez-Herrero, S., Rubio-Mediavilla, S., Narro-Íñiguez, J., & Martínez, A. (2017). Small molecules related to adrenomedullin reduce tumor burden in a mouse model of colitis-associated colon cancer. *Scientific Reports*, 7(1), 17488. doi:10.1038/s41598-017-17573-x
- Okumura, H., Nagaya, N., Itoh, T., Okano, I., Hino, J., Mori, K., . . . Kangawa, K. (2004). Adrenomedullin Infusion Attenuates Myocardial Ischemia/Reperfusion Injury Through the Phosphatidylinositol 3-Kinase/Akt-Dependent Pathway. *Circulation*, 109(2), 242-248. doi:10.1161/01.cir.0000109214.30211.7c
- Pariante, C. M., & Lightman, S. L. (2008). The HPA axis in major depression: classical theories and new developments. *Trends in Neurosciences*, 31(9), 464-468. doi:<https://doi.org/10.1016/j.tins.2008.06.006>
- Parthier, C., Reedt-Runge, S., Rudolph, R., & Stubbs, M. T. (2009). Passing the baton in class B GPCRs: peptide hormone activation via helix induction? *Trends Biochem Sci*, 34(6), 303-310. doi:10.1016/j.tibs.2009.02.004
- Pio, R., Martinez, A., Unsworth, E. J., Kowalak, J. A., Bengoechea, J. A., Zipfel, P. F., . . . Cuttitta, F. (2001). Complement factor H is a serum-binding protein for adrenomedullin, and the resulting complex modulates the bioactivities of both partners. *J Biol Chem*, 276(15), 12292-12300. doi:10.1074/jbc.M007822200
- Povsic, T. J., Kohout, T. A., & Lefkowitz, R. J. (2003).  $\beta$ -Arrestin1 Mediates Insulin-like Growth Factor 1 (IGF-1) Activation of Phosphatidylinositol 3-Kinase (PI3K) and Anti-apoptosis. *Journal of Biological Chemistry*, 278(51), 51334-51339. doi:10.1074/jbc.M309968200
- Qiao F, Fang J, Xu J, Zhao W, Ni Y, Akuo BA, Zhang W, Liu Y, Ding F, Li G, Liu B, Wang H, Shao S. (2017) The role of adrenomedullin in the pathogenesis of gastric cancer. *Oncotarget*. 2017 Jun 29;8(51):88464-88474. doi:10.18632/oncotarget.18881. eCollection 2017 Oct 24. PubMed PMID: 29179449; PubMed Central PMCID: PMC5687619.
- Riss TL, Moravec RA, Niles AL, et al. Cell Viability Assays. (2013) [Updated 2016 Jul 1]. In: Sittampalam GS, Coussens NP, Brimacombe K, et al., editors. *Assay Guidance Manual* [Internet]. Bethesda (MD): Eli Lilly & Company and the National Center for Advancing Translational Sciences; 2004-. Available from: <https://www.ncbi.nlm.nih.gov/books/NBK144065/>
- Robinson, S. D., Aitken, J. F., Bailey, R. J., Poyner, D. R., & Hay, D. L. (2009). Novel Peptide Antagonists of Adrenomedullin and Calcitonin Gene-Related Peptide Receptors: Identification, Pharmacological Characterization, and Interactions with Position 74 in Receptor Activity-Modifying Protein 1/3. *Journal of Pharmacology and Experimental Therapeutics*, 331(2), 513-521. doi:10.1124/jpet.109.156448
- Rosenblatt, M. I., Dahl, G. P., & Dickerson, I. M. (2000). Characterization and localization of the rabbit ocular calcitonin gene-related peptide (CGRP)-receptor component protein (RCP). *Invest Ophthalmol Vis Sci*, 41(5), 1159-1167.

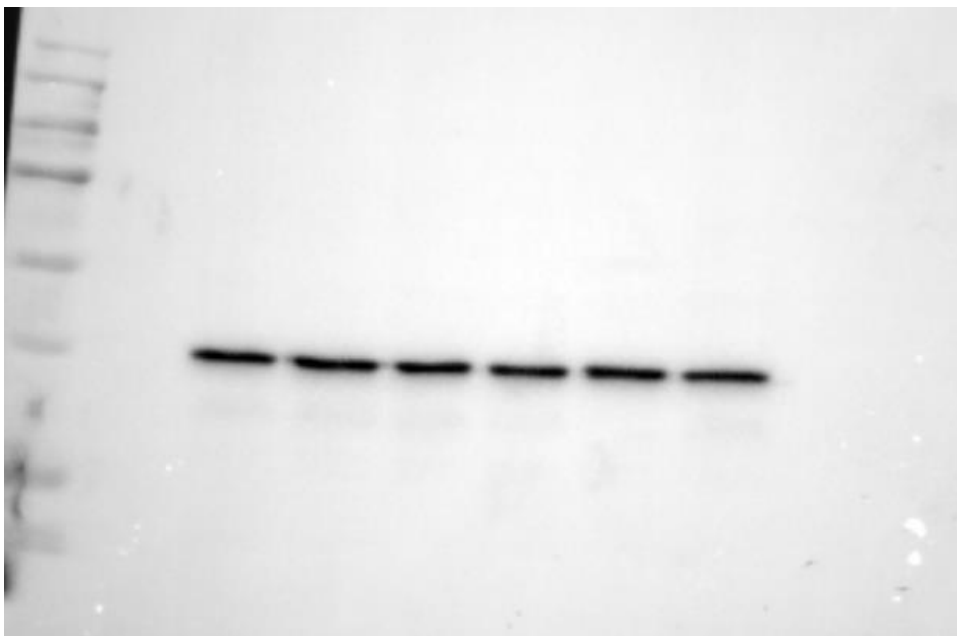
- Sata, M., Kakoki, M., Nagata, D., Nishimatsu, H., Suzuki, E., Aoyagi, T., . . . Hirata, Y. (2000). Adrenomedullin and nitric oxide inhibit human endothelial cell apoptosis via a cyclic GMP-independent mechanism. *Hypertension*, *36*(1), 83-88.
- Schwindinger, W. F., & Robishaw, J. D. (2001). Heterotrimeric G-protein betagamma-dimers in growth and differentiation. *Oncogene*, *20*(13), 1653-1660. doi:10.1038/sj.onc.1204181
- Sexton, P. M., Albiston, A., Morfis, M., & Tilakaratne, N. (2001). Receptor activity modifying proteins. *Cell Signal*, *13*(2), 73-83. doi:[https://doi.org/10.1016/S0898-6568\(00\)00143-1](https://doi.org/10.1016/S0898-6568(00)00143-1)
- Shimekake Y, Nagata K, Ohta S, Kambayashi Y, Teraoka H, Kitamura K, Eto T, Kangawa K, Matsuo H. (1995) Adrenomedullin stimulates two signal transduction pathways, cAMP accumulation and Ca<sup>2+</sup> mobilization, in bovine aortic endothelial cells. *J Biol Chem*. 1995 Mar 3;270(9):4412-7.
- Siclari, V. A., Mohammad, K. S., Tompkins, D. R., Davis, H., McKenna, C. R., Peng, X., . . . Chirgwin, J. M. (2014). Tumor-expressed adrenomedullin accelerates breast cancer bone metastasis. *Breast Cancer Res*, *16*(6), 458. doi:10.1186/s13058-014-0458-y
- Stephens, L., Smrcka, A., Cooke, F. T., Jackson, T. R., Sternweis, P. C., & Hawkins, P. T. (1994). A novel phosphoinositide 3 kinase activity in myeloid-derived cells is activated by G protein beta gamma subunits. *Cell*, *77*(1), 83-93.
- Stockert JC, Horobin RW, Colombo LL, Blázquez-Castro A. (2018) Tetrazolium salts and formazan products in Cell Biology: Viability assessment, fluorescence imaging, and labeling perspectives. *Acta Histochem*. 2018 Apr;120(3):159-167. doi: 10.1016/j.acthis.2018.02.005.
- Sun L, Zhao M, Liu M, Su P, Zhang J, Li Y, Yang X, Wu Z. (2018) Suppression of FoxO3a attenuates neurobehavioral deficits after traumatic brain injury through inhibiting neuronal autophagy. *Behav Brain Res*. 2018 Jan 30;337:271-279. doi: 10.1016/j.bbr.2017.08.042. Epub 2017 Sep 6
- Tzivion, G., Dobson, M., & Ramakrishnan, G. (2011). FoxO transcription factors; Regulation by AKT and 14-3-3 proteins. *Biochimica et Biophysica Acta (BBA) - Molecular Cell Research*, *1813*(11), 1938-1945. doi:<https://doi.org/10.1016/j.bbamcr.2011.06.002>
- Vandesompele, J., De Preter, K., Pattyn, F., Poppe, B., Roy, N., De Paepe, A. (2002). Accurate normalization of real-time quantitative RT-PCR data by geometric averaging of multiple internal control genes. *Genome Biol*. 3. 1-11.
- Varghese, F. P., & Brown, E. S. (2001). The Hypothalamic-Pituitary-Adrenal Axis in Major Depressive Disorder: A Brief Primer for Primary Care Physicians. *Primary Care Companion to The Journal of Clinical Psychiatry*, *3*(4), 151-155.
- Walker, C. S., Conner, A. C., Poyner, D. R., & Hay, D. L. (2016) Regulation of signal transduction by calcitonin gene-related peptide receptors. *Trends in Pharmacological Sciences*, *31*(10), 476-483. doi:10.1016/j.tips.2010.06.006
- Weston, C., Winfield, I., Harris, M., Hodgson, R., Shah, A., Dowell, S. J., ... Ladds, G. (2016). Receptor activity-modifying protein-directed G protein signaling specificity for the calcitonin gene-related peptide family of receptors. *Journal of Biological Chemistry*, *291*(42), 21925-21944. <https://doi.org/10.1074/jbc.M116.751362>
- Wittchen, H. U., Jacobi, F., Rehm, J., Gustavsson, A., Svensson, M., Jonsson, B., . . . Steinhausen, H. C. (2011). The size and burden of mental disorders and other disorders of the brain in Europe 2010. *Eur Neuropsychopharmacol*, *21*(9), 655-679. doi:10.1016/j.euroneuro.2011.07.018
- Xu, Y., & Krukoff, T. L. (2005). Adrenomedullin stimulates nitric oxide release from SK-N-SH human neuroblastoma cells by modulating intracellular calcium mobilization. *Endocrinology*, *146*(5), 2295-2305. doi:10.1210/en.2004-1354
- Yen, D. H. T., Chen, L.-C., Shen, Y.-C., Chiu, Y.-C., Ho, I. C., Lou, Y.-J., . . . Yen, J.-C. (2011). Protein kinase A-dependent Neuronal Nitric Oxide Synthase Activation Mediates the Enhancement of Baroreflex Response by Adrenomedullin in the Nucleus Tractus Solitarii of Rats. *Journal of Biomedical Science*, *18*(1), 32-32. doi:10.1186/1423-0127-18-32
- Yoshimoto, T., & Hirata, Y. (2005). Adrenomedullin Receptor and Signal Transduction. In T. Nishikimi (Ed.), *Adrenomedullin in Cardiovascular Disease*. United States of America: Springer.

Zeng, Z., Wang, X., Bhardwaj, S. K., Zhou, X., Little, P. J., Quirion, R., . . . Zheng, W. (2017). The Atypical Antipsychotic Agent, Clozapine, Protects Against Corticosterone-Induced Death of PC12 Cells by Regulating the Akt/FoxO3a Signaling Pathway. *Molecular Neurobiology*, 54(5), 3395-3406. doi:10.1007/s12035-016-9904-4

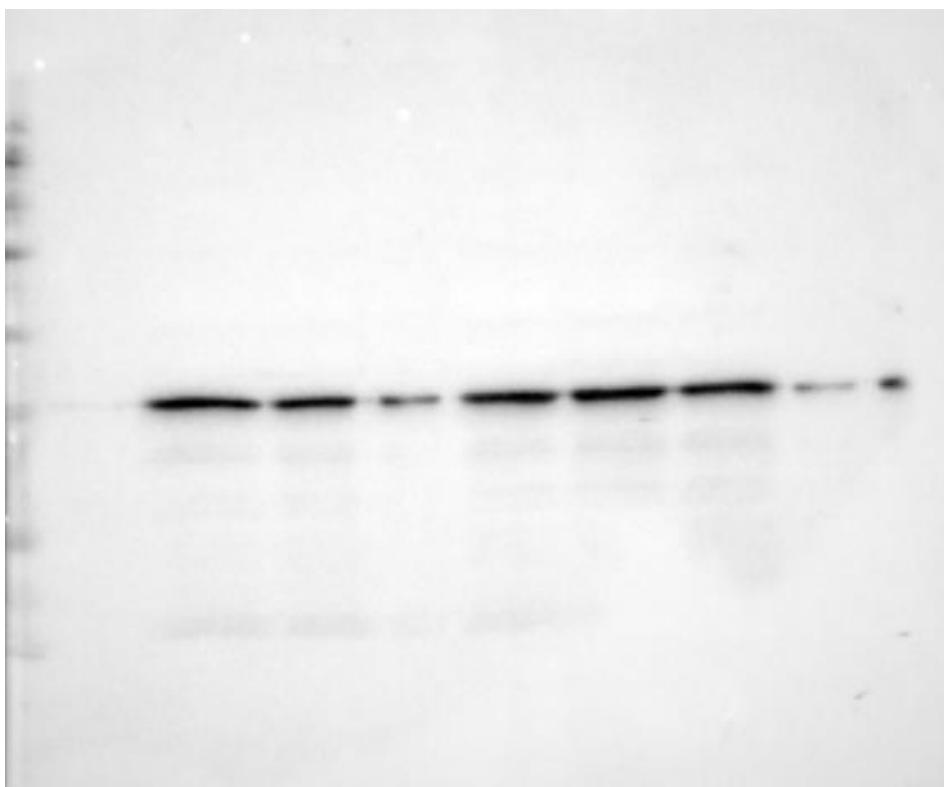
## Appendices



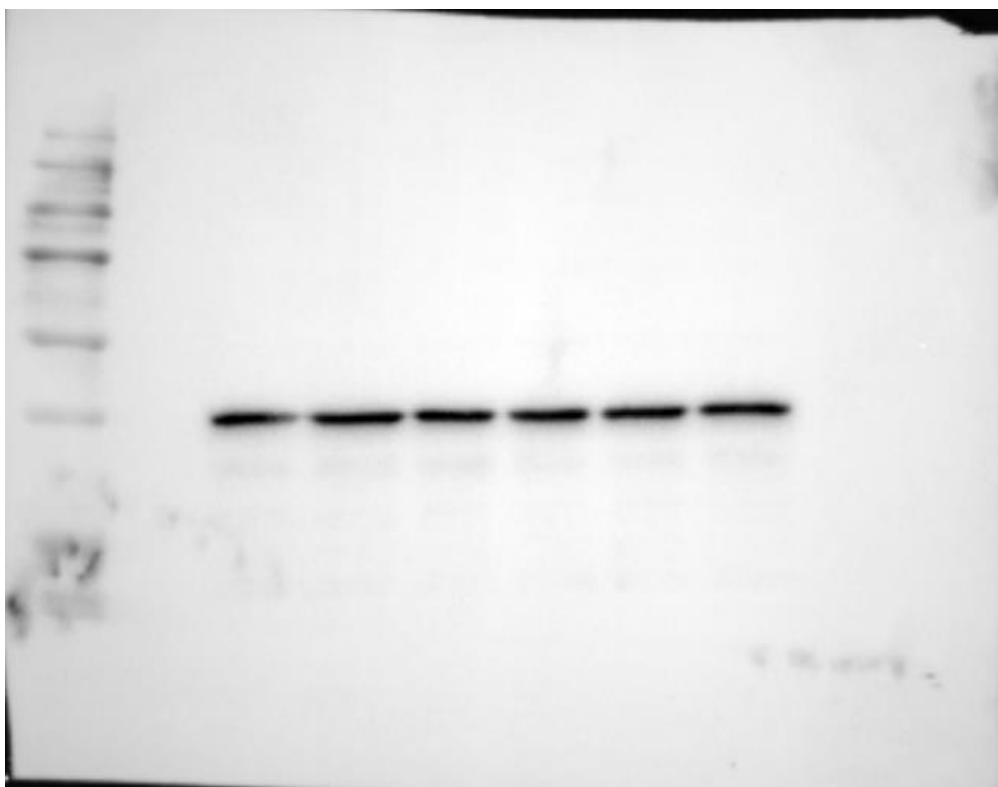
A1) Western blot showing bands corresponding to GAPDH for samples 1-6 of the FoxO3a antibody treated blot shown as blot a, Figure 3.6.



A2) Western blot showing bands corresponding to GAPDH for samples 7-12 of the FoxO3a antibody treated blot shown as blot b, Figure 3.6.



**A3) Western blot showing bands corresponding to GAPDH for samples 1-6 of the P-FoxO3a antibody treated blot shown in blot c, Figure 3.7.**



**A4) Western blot showing bands corresponding to GAPDH for samples 7-12 of the P-FoxO3a antibody treated blot shown in blot d, Figure 3.7.**

